The Effect of Defects and Surface Modification on Biomolecular Assembly and Transport

SAND2019-3292PE

Haneen Martinez

Candidate for Ph.D. Nanoscience and Microsystems Engineering

University of New Mexico

Dissertation Defense

March 13th, 2019

Dissertation Committee: Dr. Andrew P. Shreve, Dr. George D. Bachand, Dr. Nick J. Carroll, and Dr. Francesca Cavallo

Self-assembly

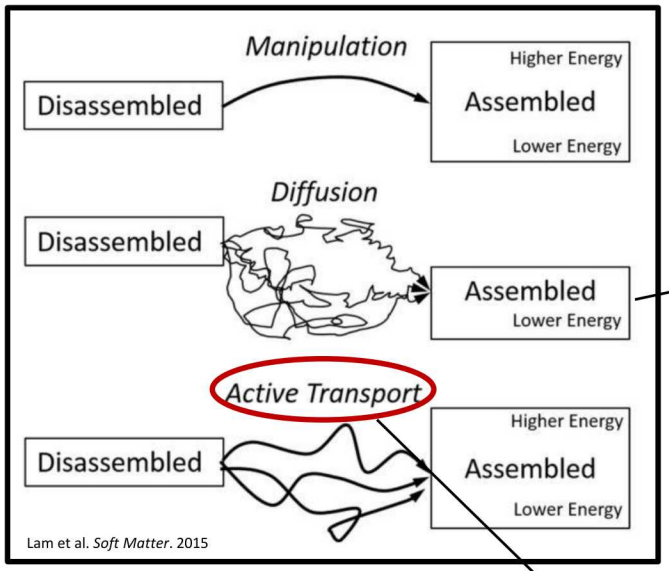

Lam et al. *Soft Matter*. 2015

DNA origami

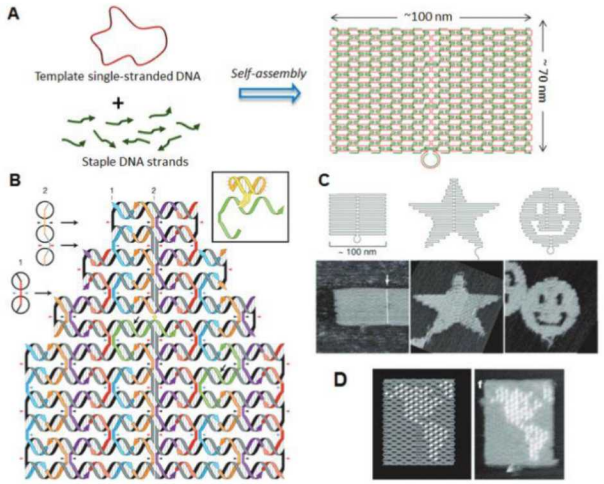

Endo et al. Biom. Sci. 2012

Biological processes use active-self assembly to overcome limitations of diffusion

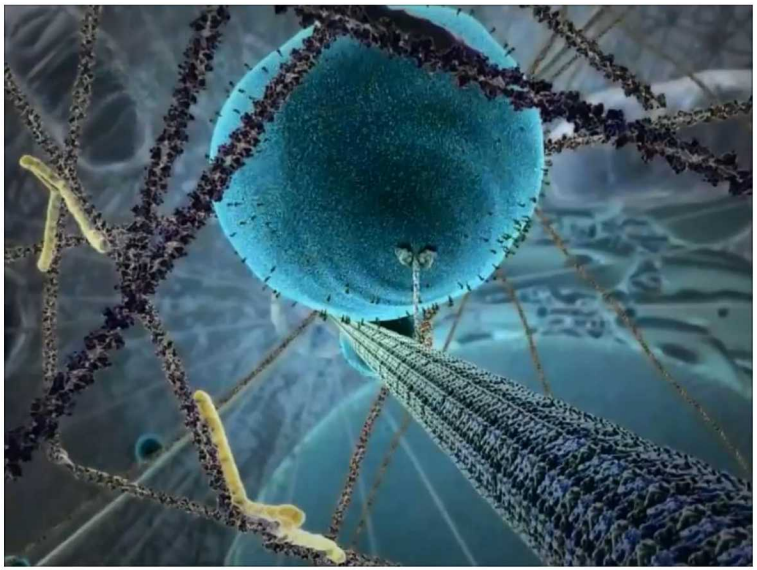
"The inner life of a cell"; https://www.youtube.com/watch?v=y-uuk4Pr2i8

Microtubule cytoskeletal filaments

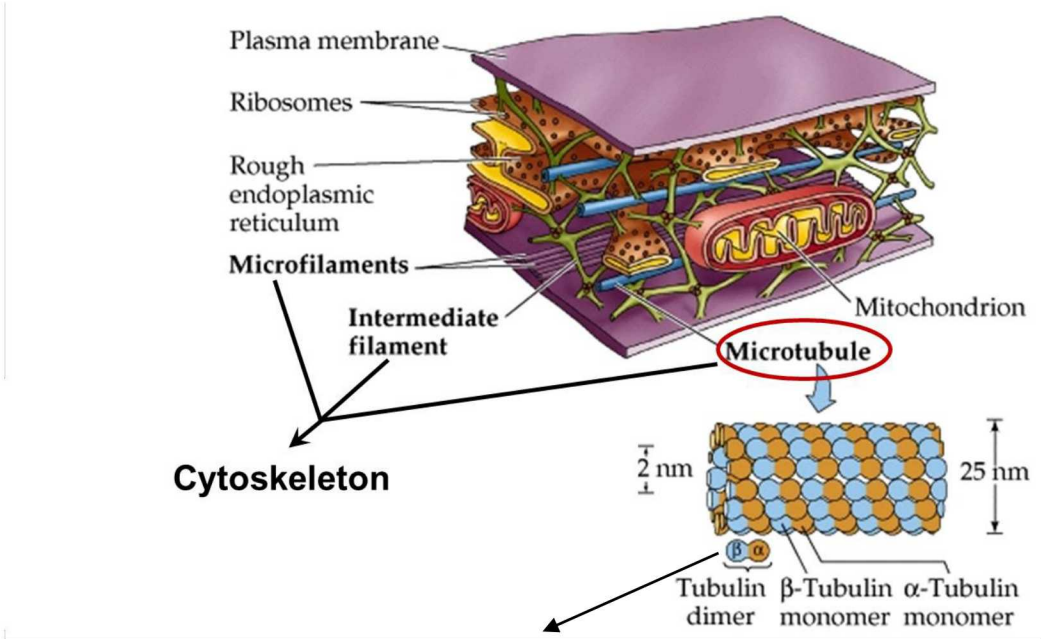

http://www.slideshare.net/hphuonglinh/11-cell-structure

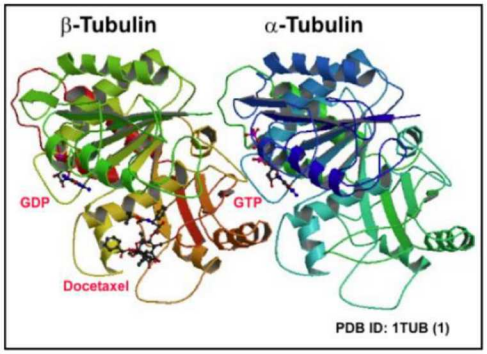

https://www.embrn.eu/resources/wiki/microtubules-and-mast-cell-signaling.html

- Microtubules (MTs) are polymeric filaments
  - Provide structural support for the cell
  - Act as intracellular network for motor protein transport
- MTs are made of α,β-tubulin dimers
  - 55 kDa
  - Both bind GTP, but only β- can hydrolyze to GDP

MT formation and dynamic instability

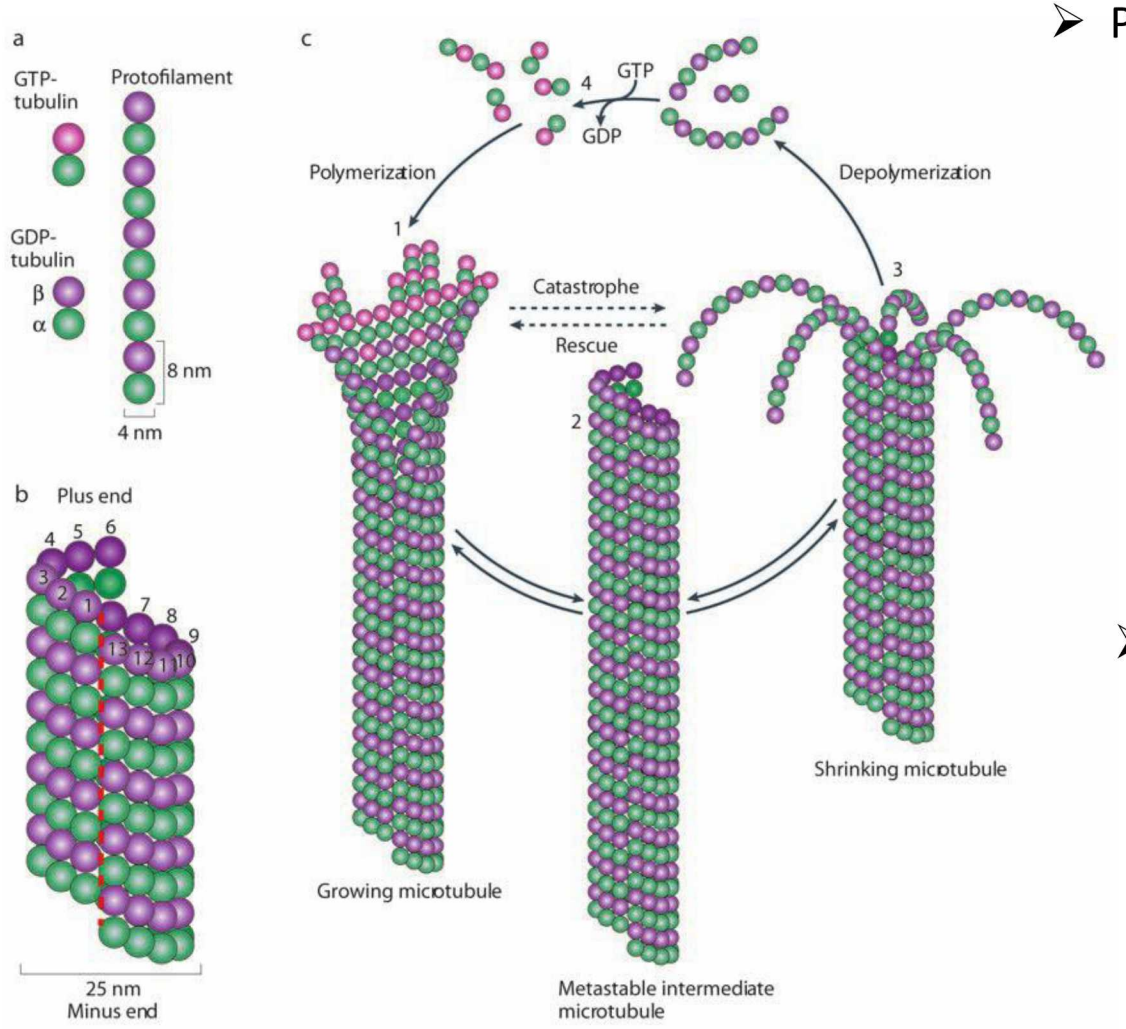

- Polymerization of MTs:
  - tubulin dimers bind together in a head-to-tail fashion
  - dimers elongate into protofilaments
  - protofilaments interact laterally to form sheets and eventually close into a hollow tube
- MTs grow and shrink with abrupt transitions between the phases, a phenomenon known as “dynamic instability”

Kinesin molecular motors

- Kinesins are MT-associated motors
- "Walk" hand-over-hand toward β end of microtubules (8 nm step size)
- Convert chemical energy (ATP) to mechanical work (40 pN nm) with high catalytic efficiency (>50%)

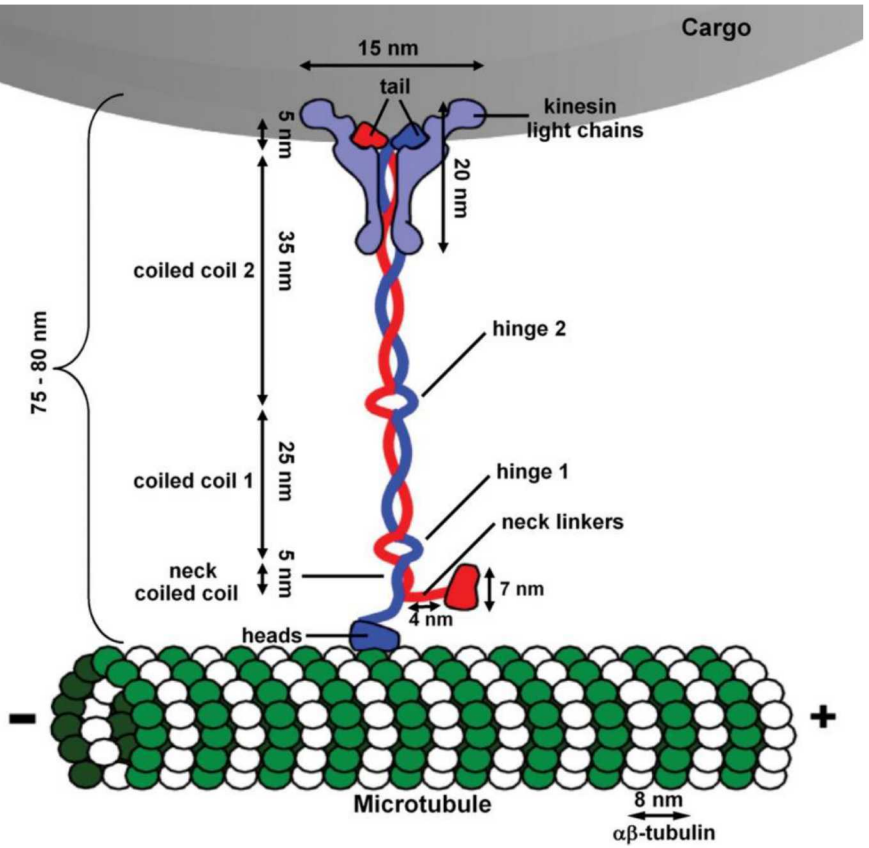

Kinesin-MT characteristics inspired their application outside of cells to create materials/systems that mimic nature

In vitro gliding assay

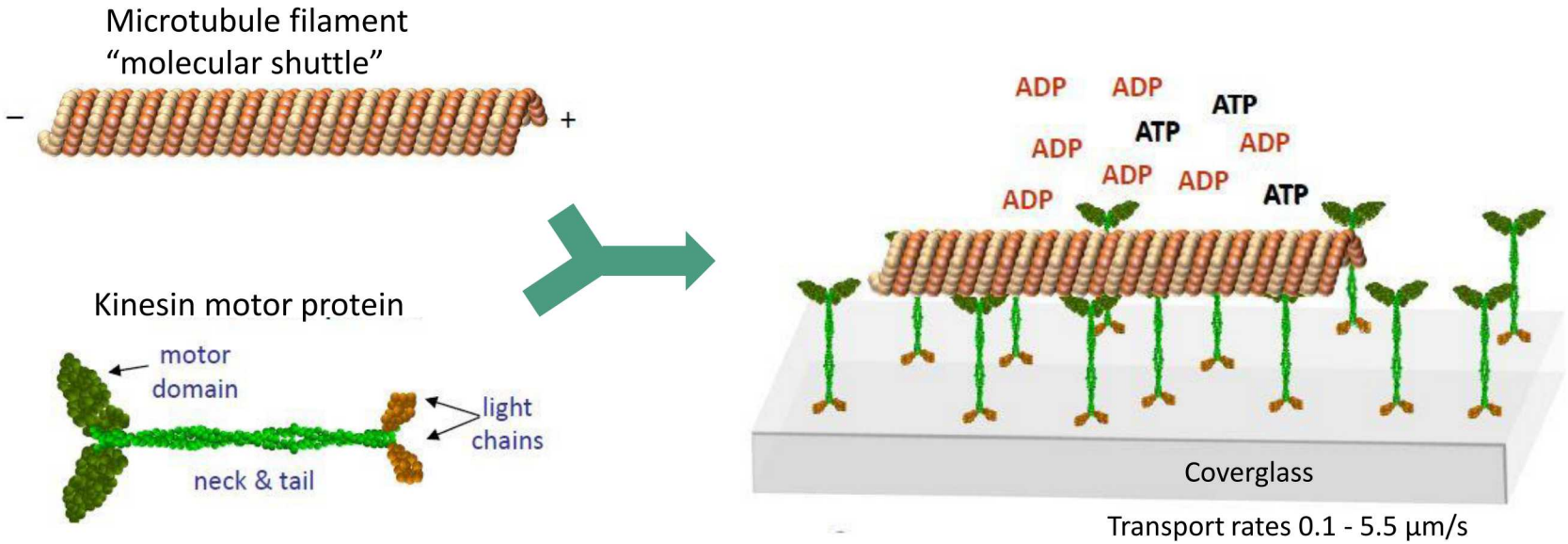

- Kinesin motors are immobilized on surface and motor heads transport the filaments through ATP hydrolysis
- This geometry enables "long distance" transport at the nanoscale

Active self -assembly using Kinesin-MT transport system

Cross-linkers enable the self-assembly of structures that differ in shape and size using the kinesin-MT system

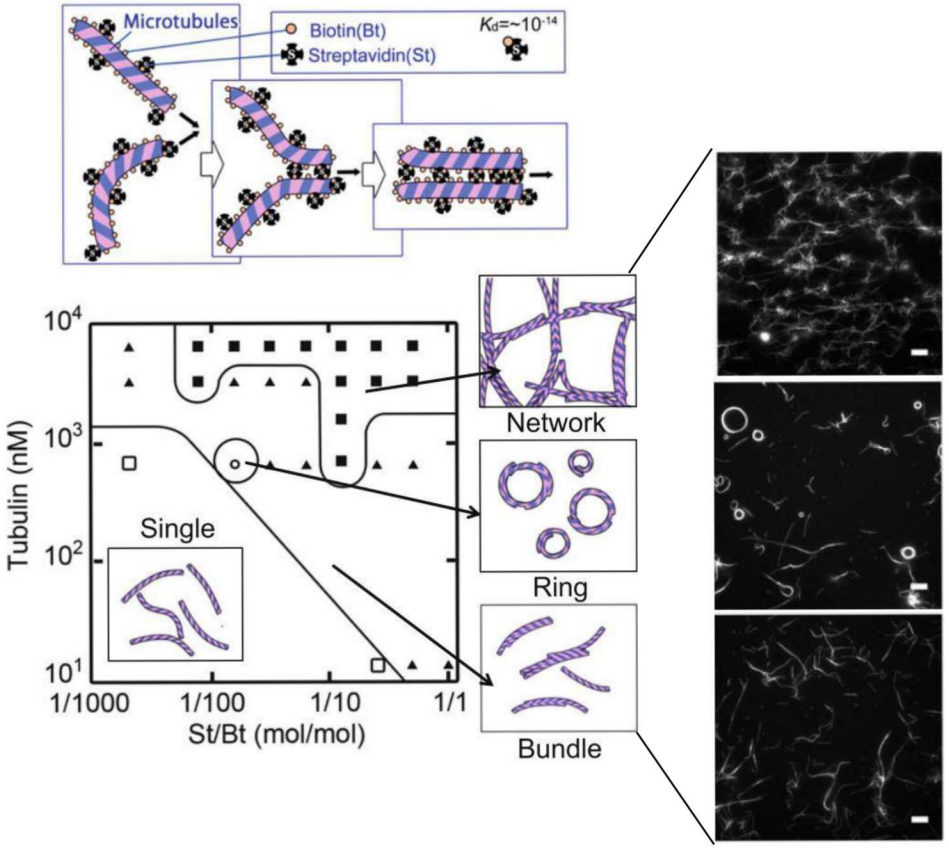

- Non-equilibrium ring structures store considerable amount of energy and provide continuous amount of work
- Understanding factors that could affect their properties is important for future nanotechnological applications

Spools have nano- and micron- scale defects

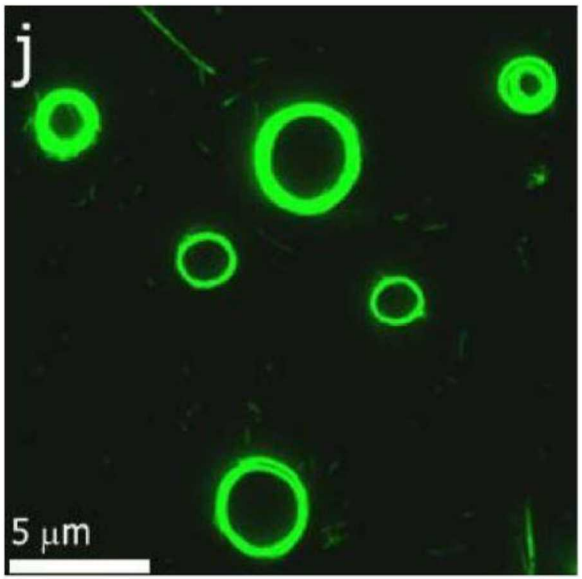

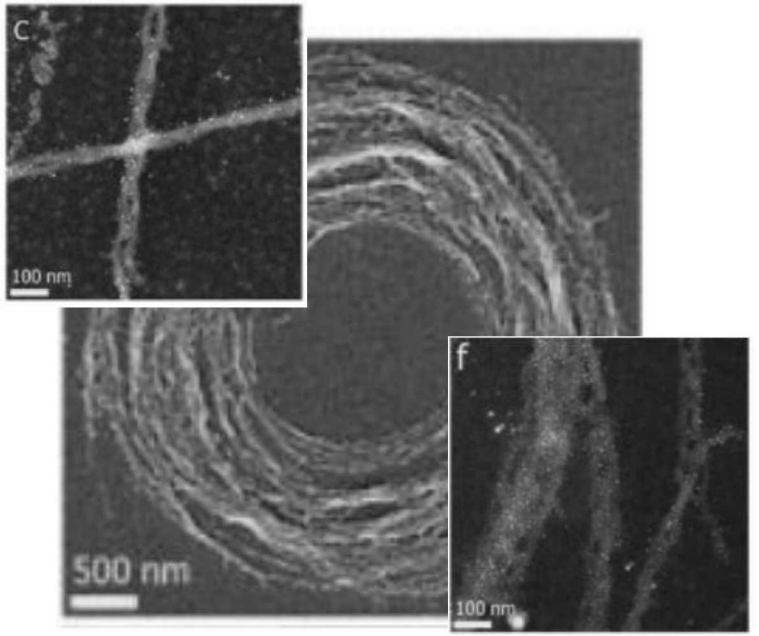

- Spools actively assembled using biotinylated MTs and streptavidin coated quantum dots (sQDs)
- Fluorescence microscopy suggests spools are well-ordered

Electron microcopy revealed structural defects:

- Twisted and kinked domains
- In- plane and out-of-plane loops
- "breakage" and release of individual MTs from spools due to structural heterogeneity

How do large (micron-scale) defects affect spool formation and stability?

Liu et al., Advanced Materials, 2008

Generating building blocks with non-bonding "defective" MT domains

Segmented MTs were generated by mixing biotinylated (blue) and non-biotinylated (green) MTs at different percentages

- Blue MT= bonding and "compliant"
- Green MT = non-bonding and "defective"

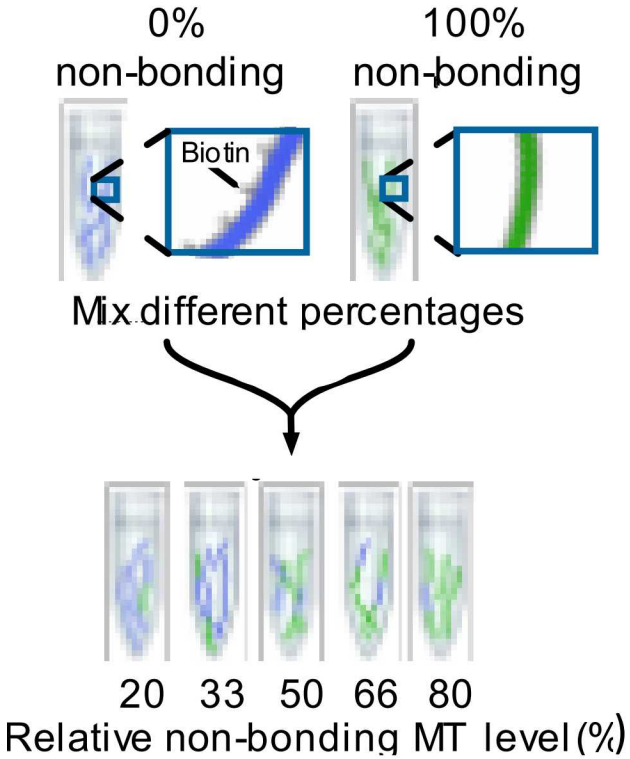

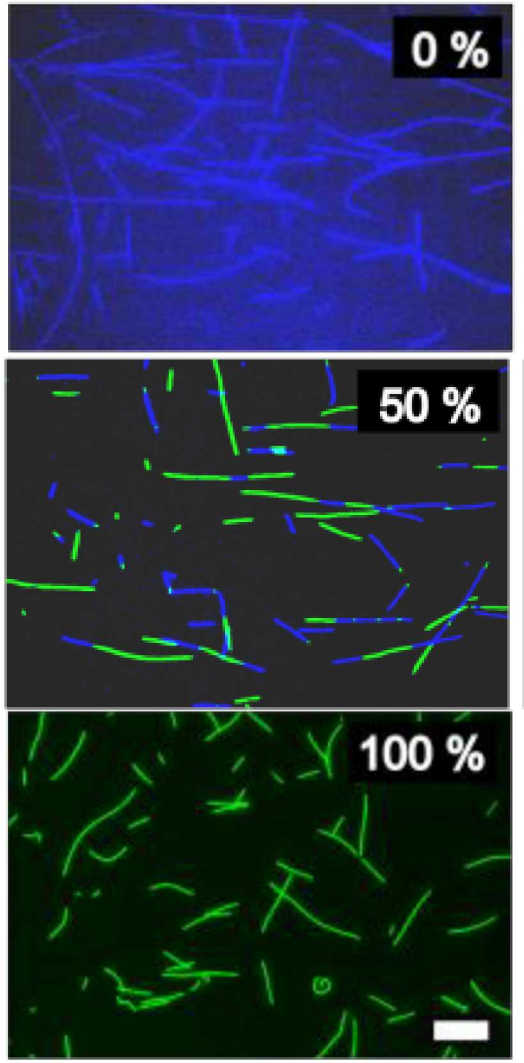

Self-assembly of Segmented MT spools

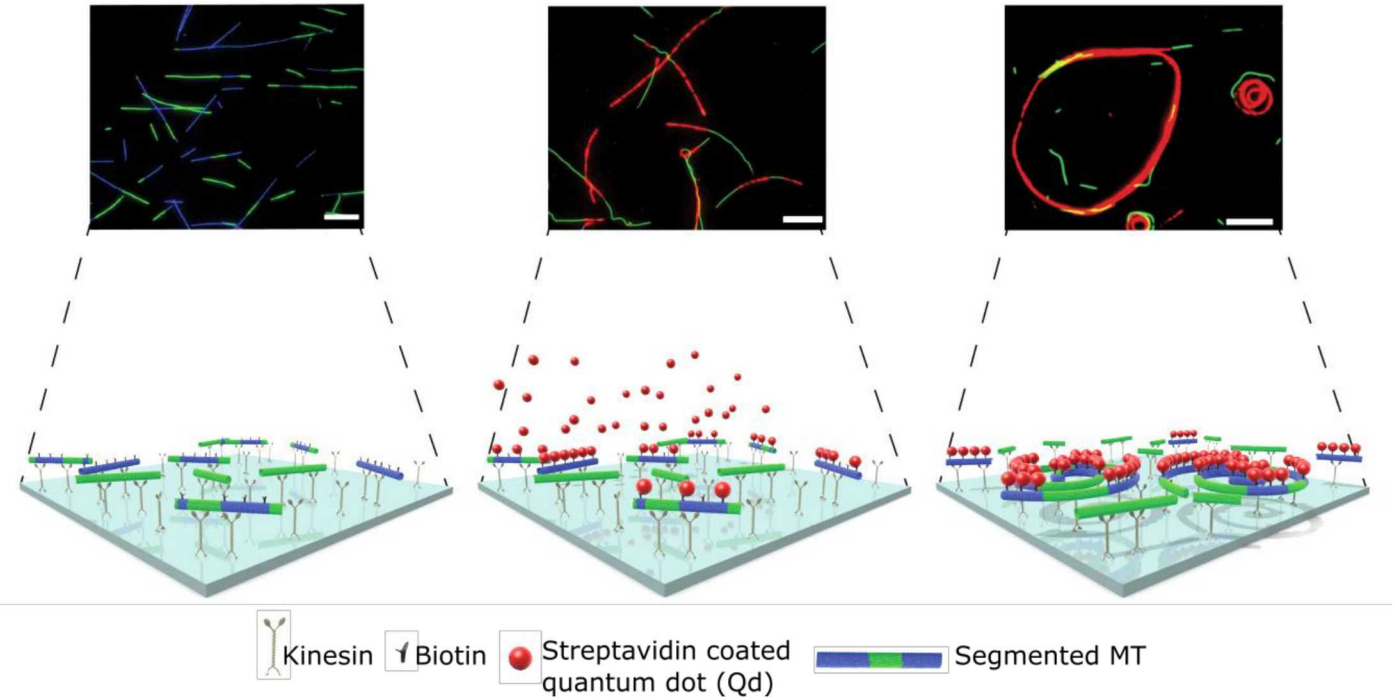

Gliding motility assay used to assemble spools

- Surface-bound kinesin motors attach and translate MTs (ATP hydrolysis)
- Spools formed through non-covalent interactions between bonding MT domains and streptavidin-coated Qds

Spool morphology depends on non-bonding MT level

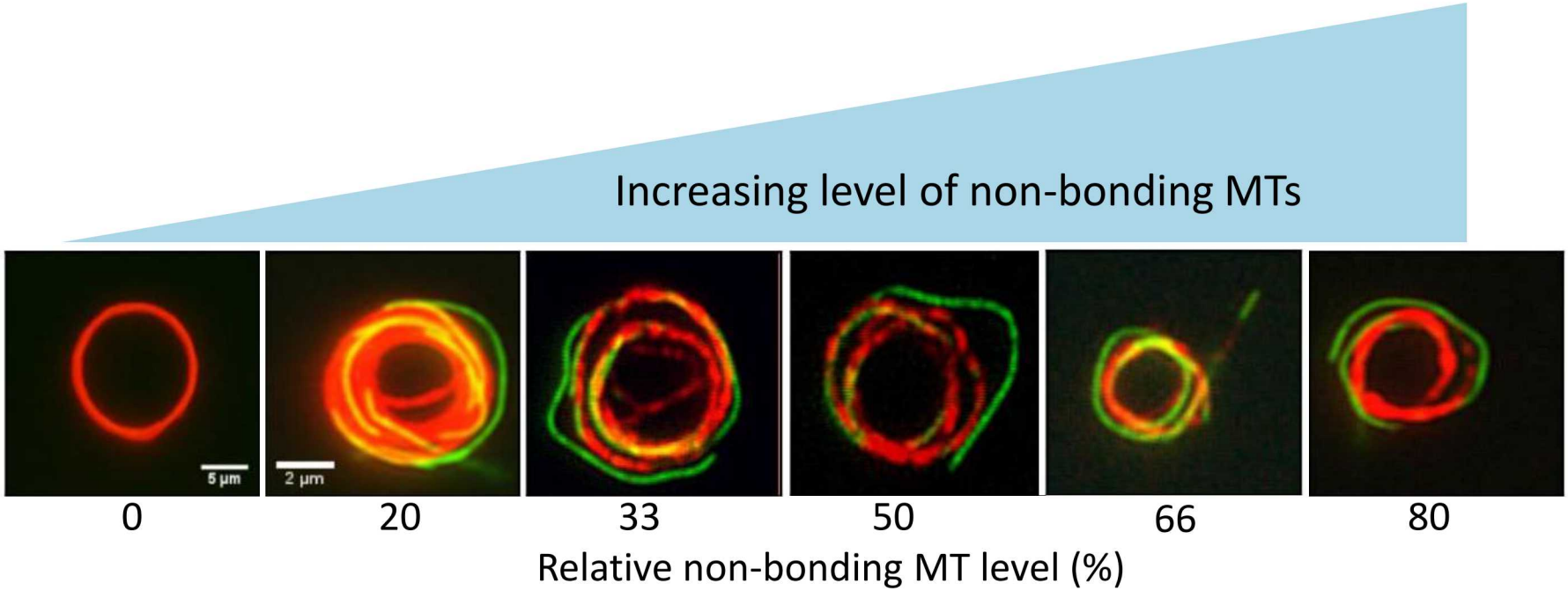

- Less densely packed structures
- larger gaps and loops
- “Hanging tails”

non-bonding bonding segmented

Spool density depended on non-bonding MT level

Density (i.e. number of spools per area) depends on availability of bonding MTs capable of nucleating the formation of a spool

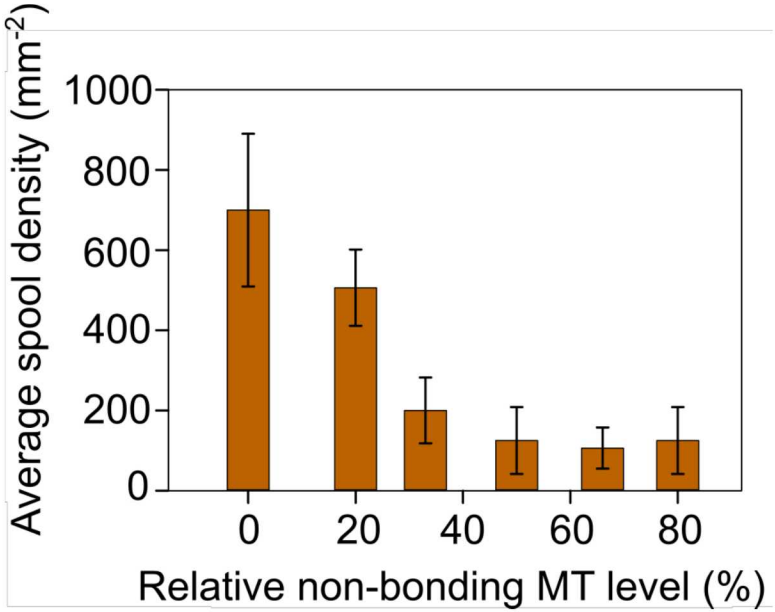

- Decrease in density of spools that formed using segmented MTs (20-80%)
- Density of spools showed an inverse correlation with non-bonding MT level

Spool initiation mechanisms

1) Pinning - MT leading tip encounters inactive/dead motor

2) Collisions -Three or more MTs collide and form polygon that evolves into ring (dominant mechanism)

3) Induced curvature – MTs travel in persistent curved trajectory until the ends interact to form a closed spool

Pinning

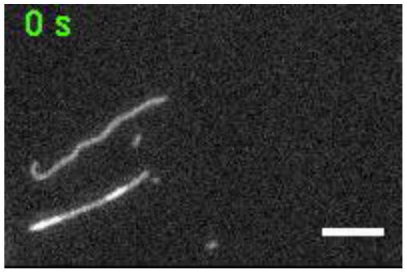

Collision

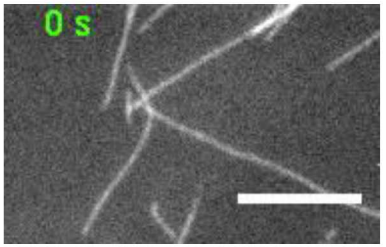

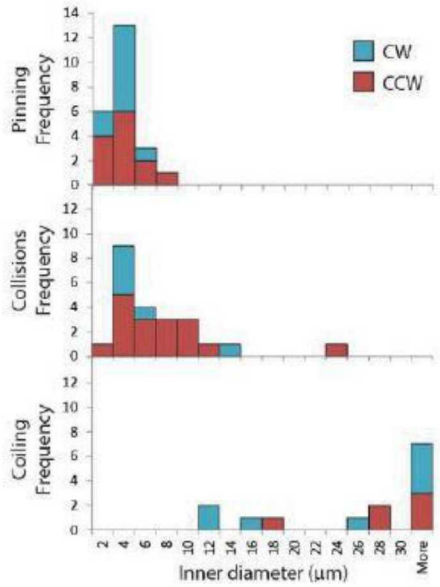

Mean diameter

2.7 ± 1.5 μm

6.2 ± 4.8 μm

32 ± 19 μm

Induced curvature

VanDelinder et al., Biomacromolecules 2016

Effect of non-bonding MT level on spool properties

Inner diameter depends on initiation mechanism (pinning, collisions, and induced curvature)

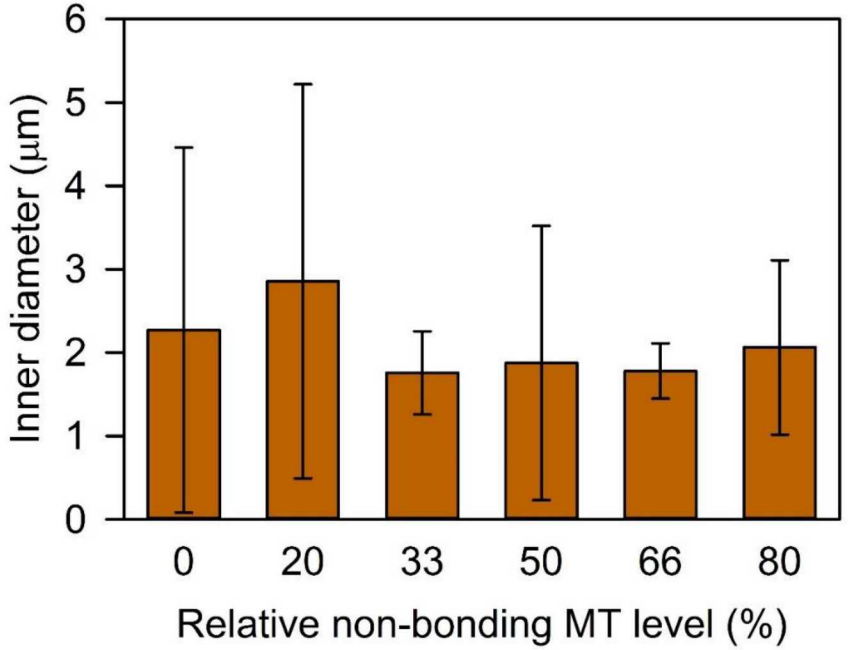

- Average inner diameter of spools for bonding (0%) and segmented (20-80%)MTs were similar
- Spools assembled by a combination of pinning and simultaneous collisions

Effect of non-bonding MT level on spool properties

- Growth of spools characterized by area
  - Colliding MTs add to the outer perimeter of spools
  - Loss of MTs from spools

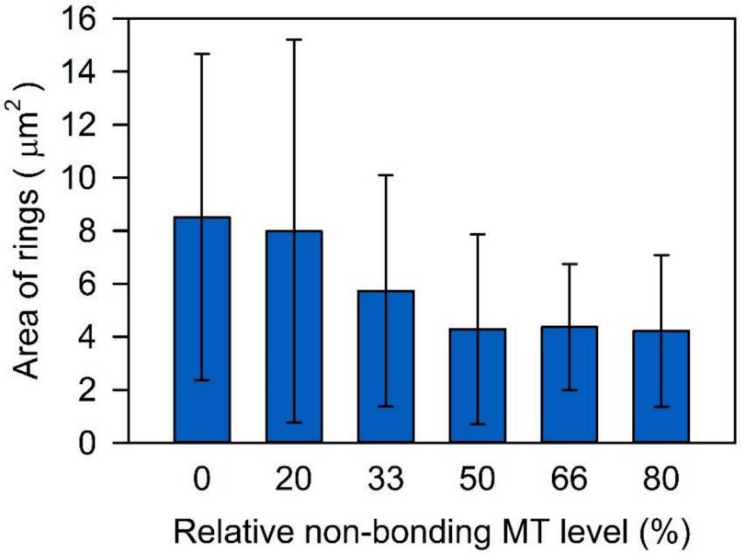

- Average area of spools formed by segmented MTs (20-80%) were <u>smaller</u> than spools formed by bonding MTs (0%)
- Area of spools <u>inversely correlated</u> with the non-bonding MT level

Non-bonding MTs hinder growth of spools

Fraction of non-bonding MTs in spools

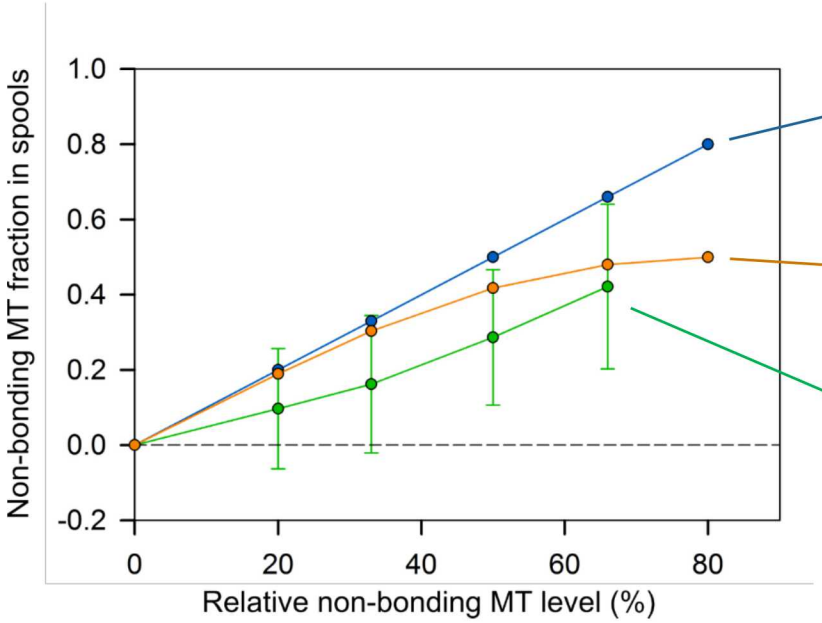

All three MT types incorporated into spools at equivalent rate

Only bonding and segmented MTs incorporated into spools

Measured fraction of non-bonding MTs in spools

non-bonding bonding segmented

Fraction of non-bonding MTs in spools

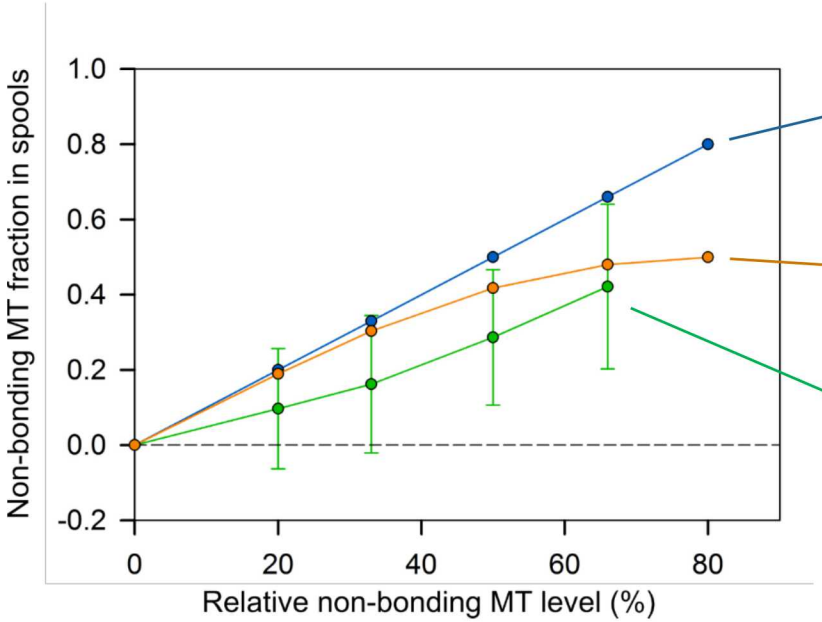

All three MT types incorporated into spools at equivalent rate

Only bonding and segmented MTs incorporated into spools

Measured fraction of non-bonding MTs in spools

Measured fraction of non-bonding MTs (green line) deviated from both theoretical predictions (blue and orange line)

Fraction of non-bonding MTs in spools

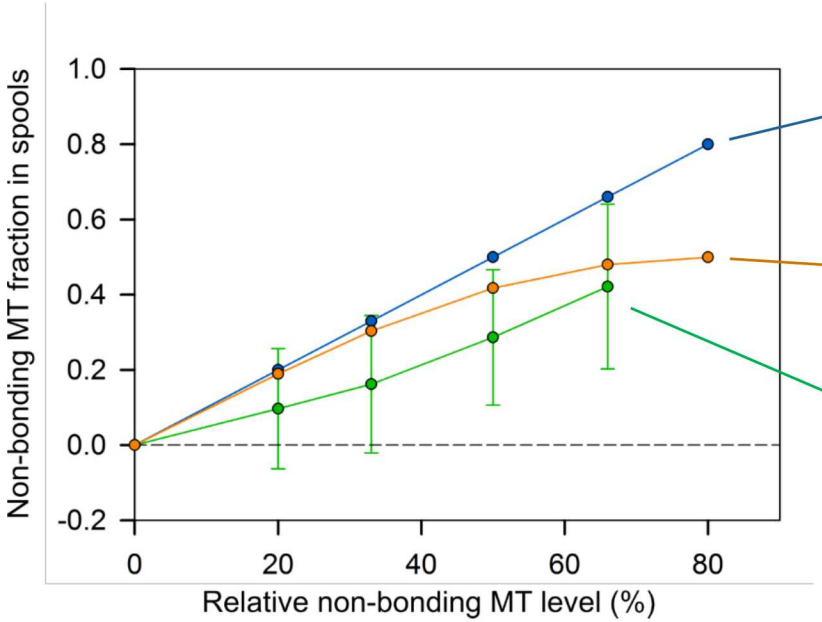

All three MT types incorporated into spools at equivalent rate

Only bonding and segmented MTs incorporated into spools

Measured fraction of non-bonding MTs in spools

Measured fraction of non-bonding MTs (green line) deviated from both theoretical predictions (blue and orange line)

- Non-bonding domains in segmented MTs = lower frequency of incorporation
- Inability of non-bonding MTs to balance high bending energy with non-covalent bond formation
- Mismatch in kinesin motor velocities causes mechanical strain

Breakage and release of non-bonding MTs

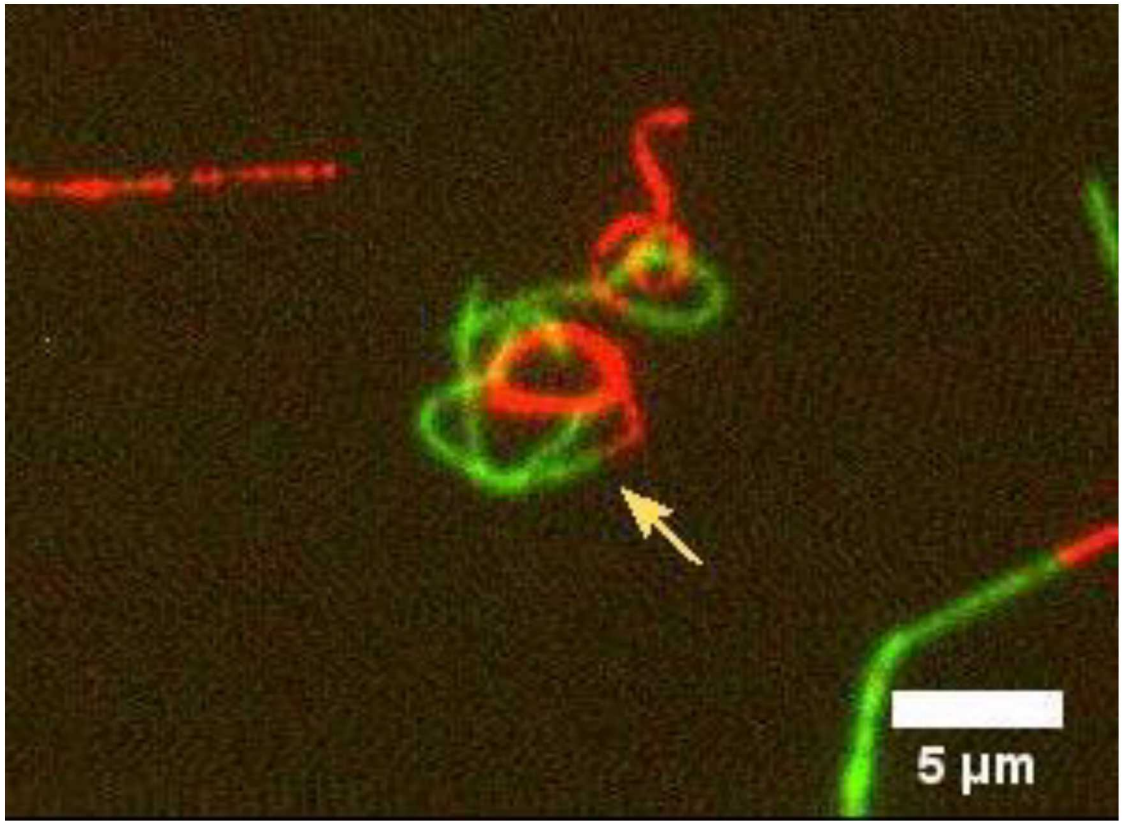

non-bonding bonding segmented

Breakage and release of non-bonding MTs

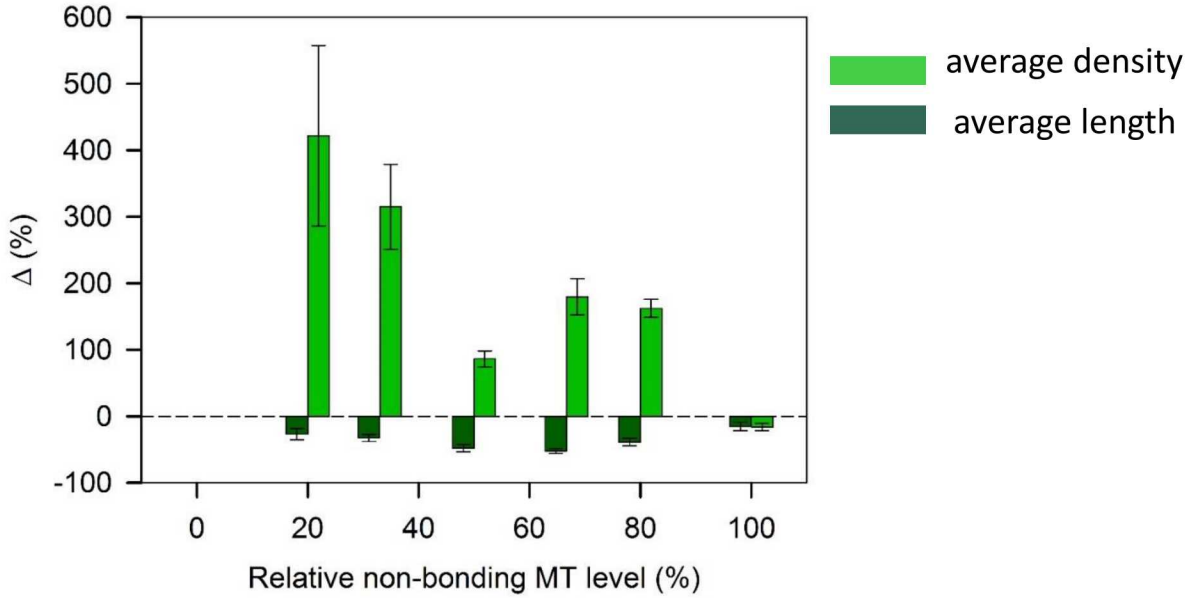

- Increase of ~ 190% in the number of non-bonding MTs (20-80%; t= 30min)

  Segmented MTs are broken into bonding and non-bonding MTs, where non-bonding MTs are preferentially released from spools

non-bonding bonding segmented

Breakage and release of non-bonding MTs

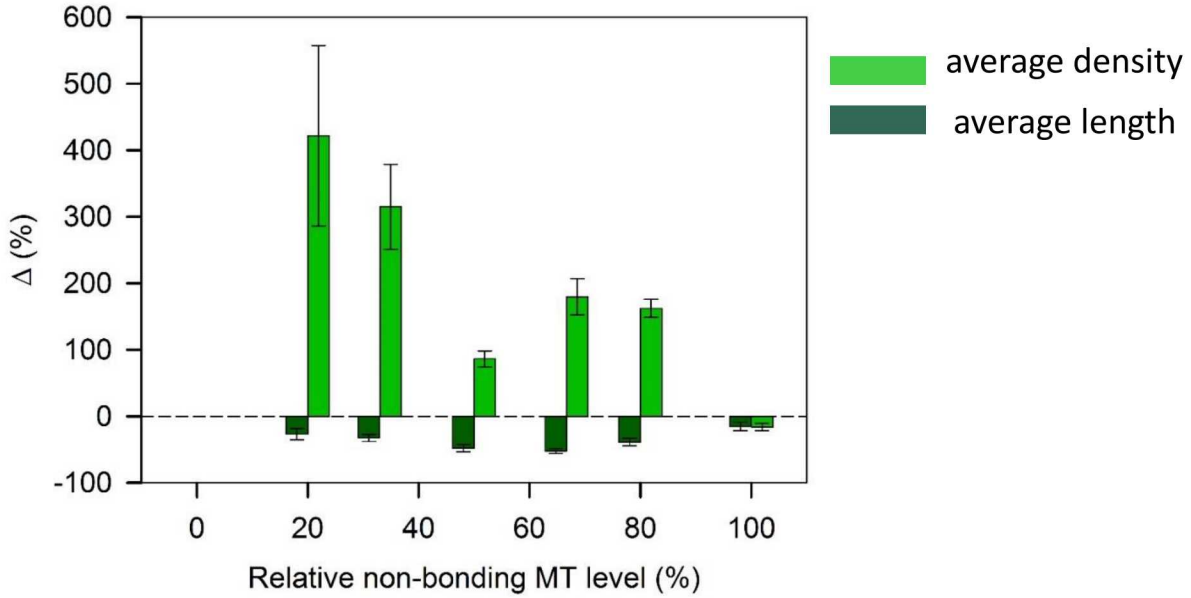

- Increase of ~ 190% in the number of non-bonding MTs (20-80%; t= 30min)

  Segmented MTs are broken into bonding and non-bonding MTs, where non-bonding MTs are preferentially released from spools

- Decrease of ~ 36% in length

  Breakage can occur at interface of non-bonding and bonding domains, as well as in the middle of non-bonding domains

non-bonding bonding segmented

Spools integrate and release MTs during growth process

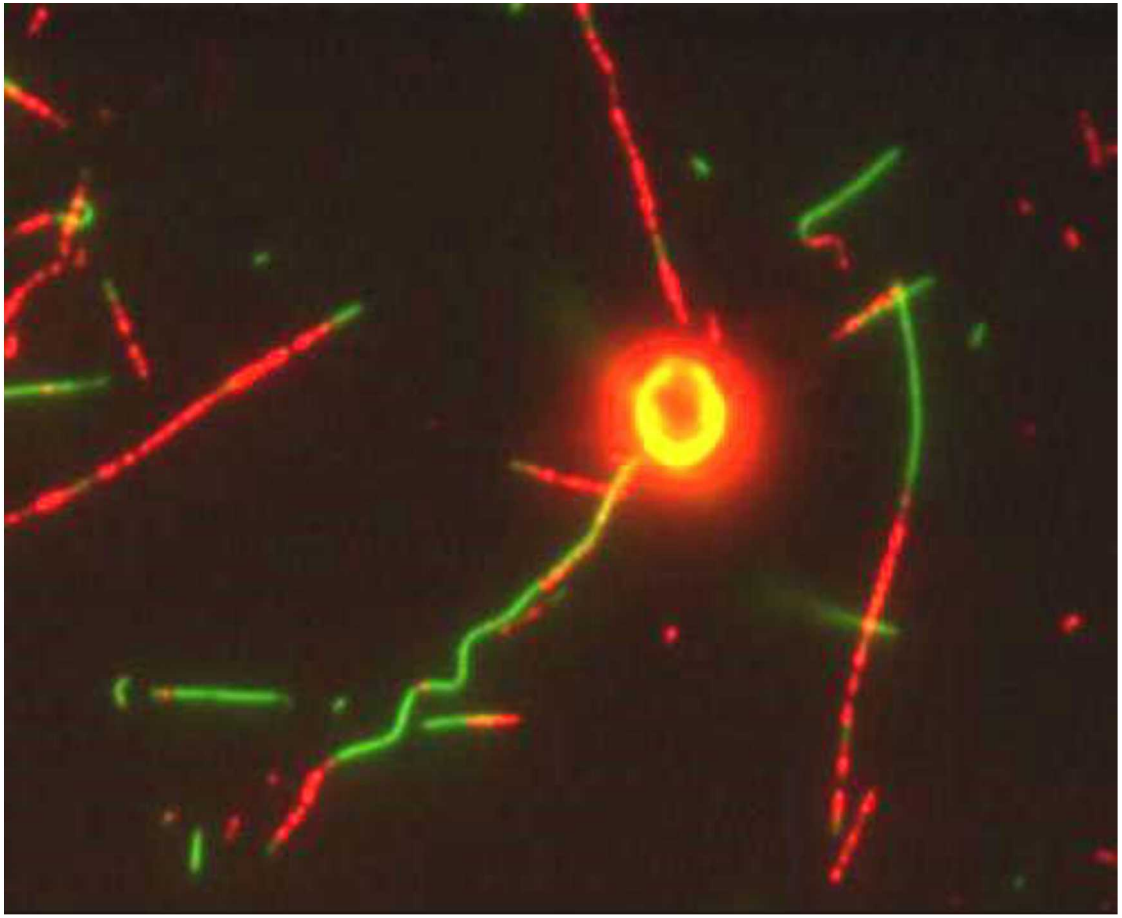

non-bonding bonding segmented

Spools integrate or reject MTs upon collision

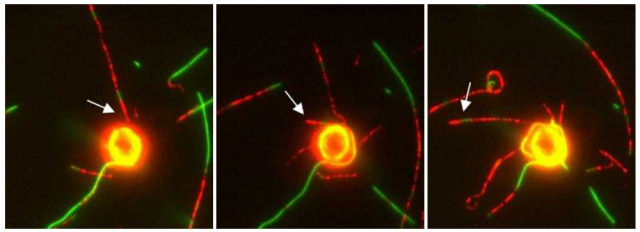

Bonding MT rejected by spool

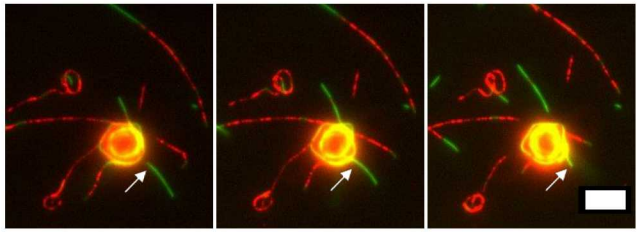

Non-bonding MT integrated into spool

non-bonding bonding segmented

Spools integrate or reject MTs upon collision

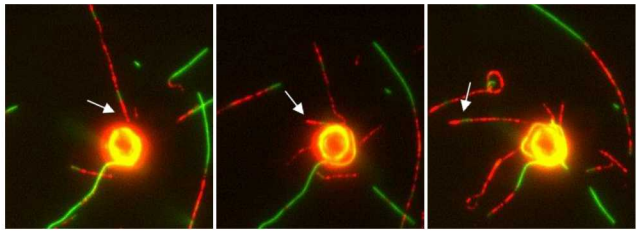

Bonding MT rejected by spool

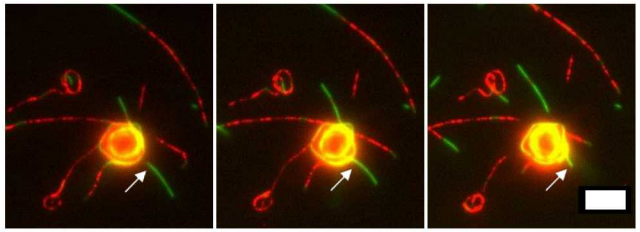

Non-bonding MT integrated into spool

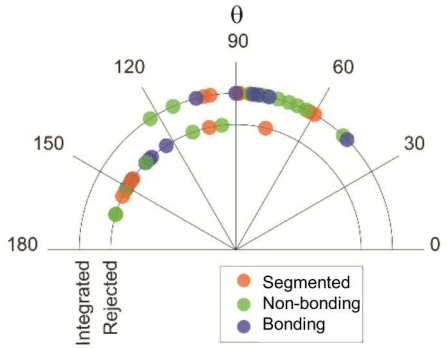

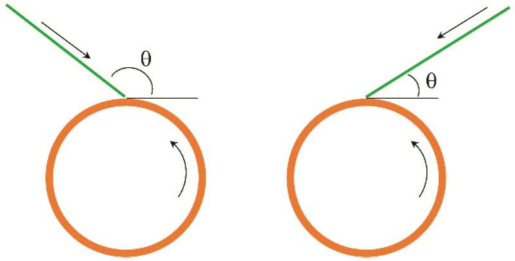

- Incorporation and rejection of all three types of MT building blocks depended on collision angle
- Incorporation of non-bonding MTs is transient (sterically trapped in gaps/loops of spool)

Conclusions

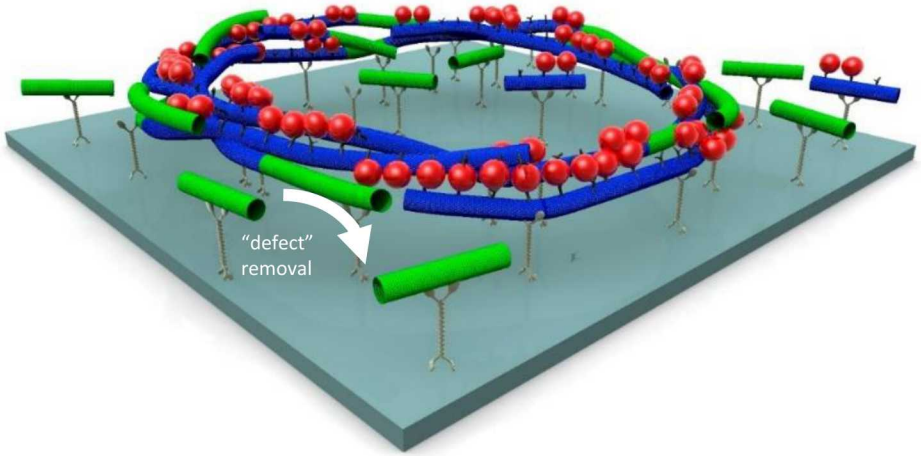

- Stable spools assembled by kinesin motors consisting of segmented building blocks that contained defective MT domains
- Spools with altered morphologies, reduced densities and areas
- Preferential removal of non-bonding domains from spools over time
- Incorporation of free MTs into spools depended on the collision angle ($\theta < 90°$)

non-bonding bonding segmented

Guiding molecular shuttles

Surface topography

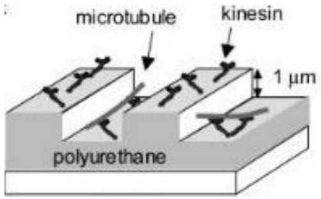

Clemmens et al, 2003

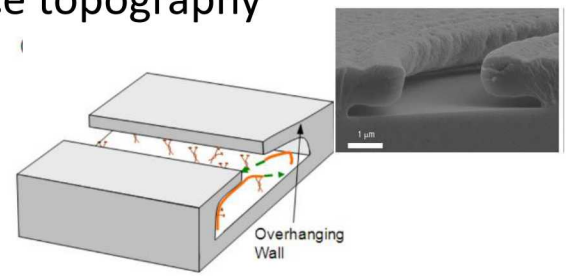

surface chemistry

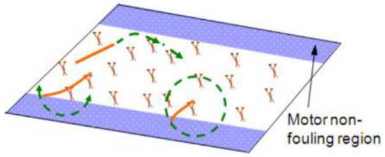

surface topography and chemistry

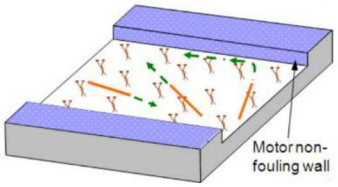

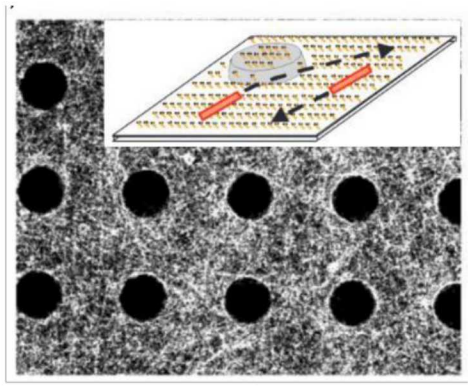

surface probing and characterization

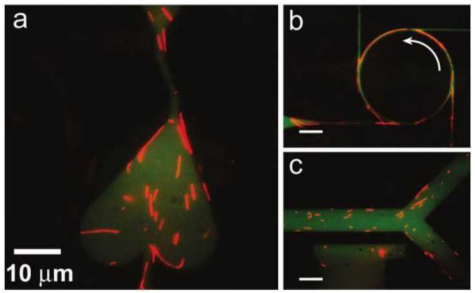

Heuvel et al, 2005

unidirectional movement on “rectifier” tracks

lithographically patterning physical and chemical features limit:

- MT trajectories by getting stuck on structures and block transport paths
- MTs escape the barriers and lead to stalling or complete loss of MTs

Need to explore more compatible substrates for reliable MT transport

Self-assembled monolayers (SAMs)

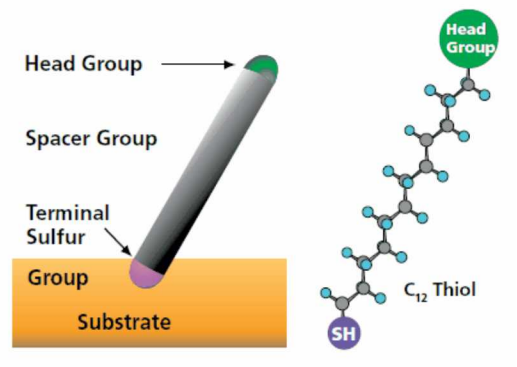

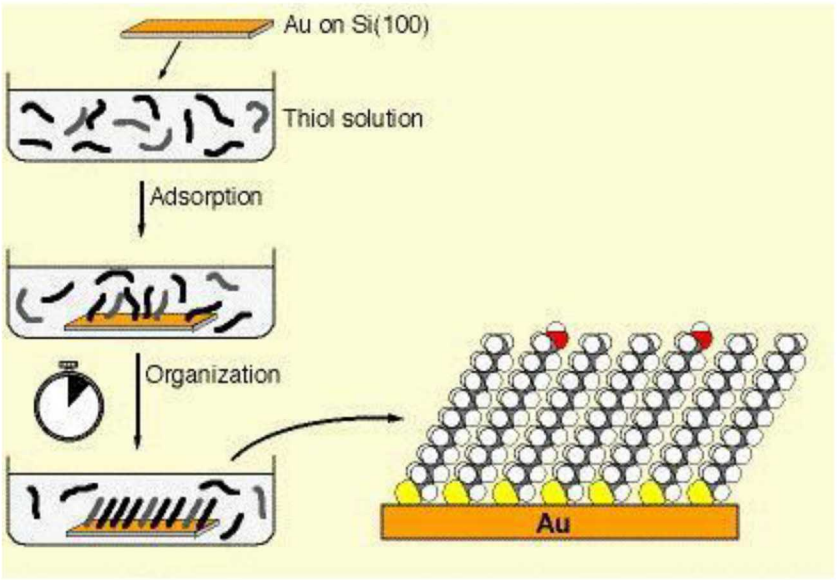

- Long chain, functionally terminated alkanthiols (HS-(CH_2)n – X, n ≥ 10) adsorb to gold surfaces
- Alkyl chains pack together to form stable, well –packed, and ordered monolayers

Head group provides a platform in which any desired group can be used to produce surfaces of any type of chemistry


Cover glass

- Chromium adhesion layer for gold
- Gold used to attach SAMs to surface

Concentration: 1 mM / Ethanol

R=	Functional Group	Characteristics
	CH_3	Neutral & Hydrophobic
	COO^-	Negatively (-) charged @ pH 7.4
	NH_3^+	Positively (+) charged @ pH 7.4

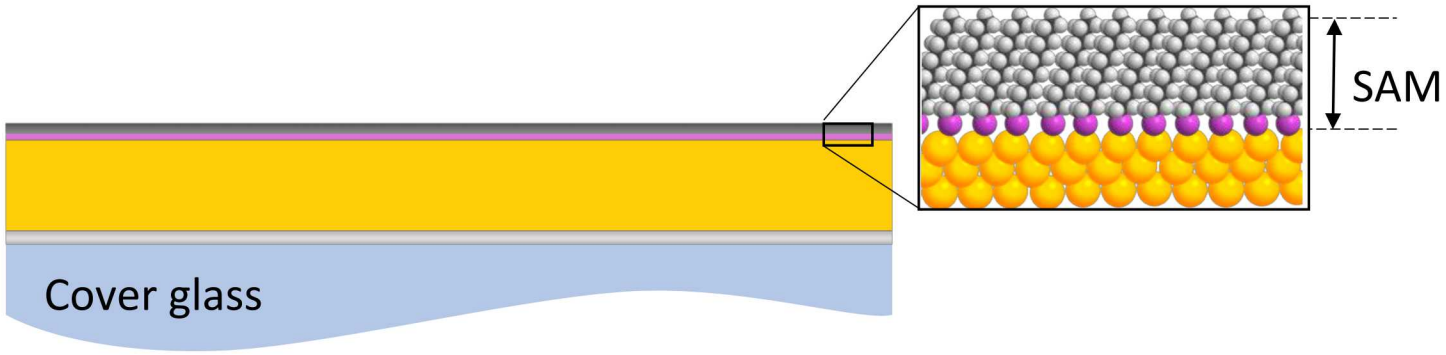

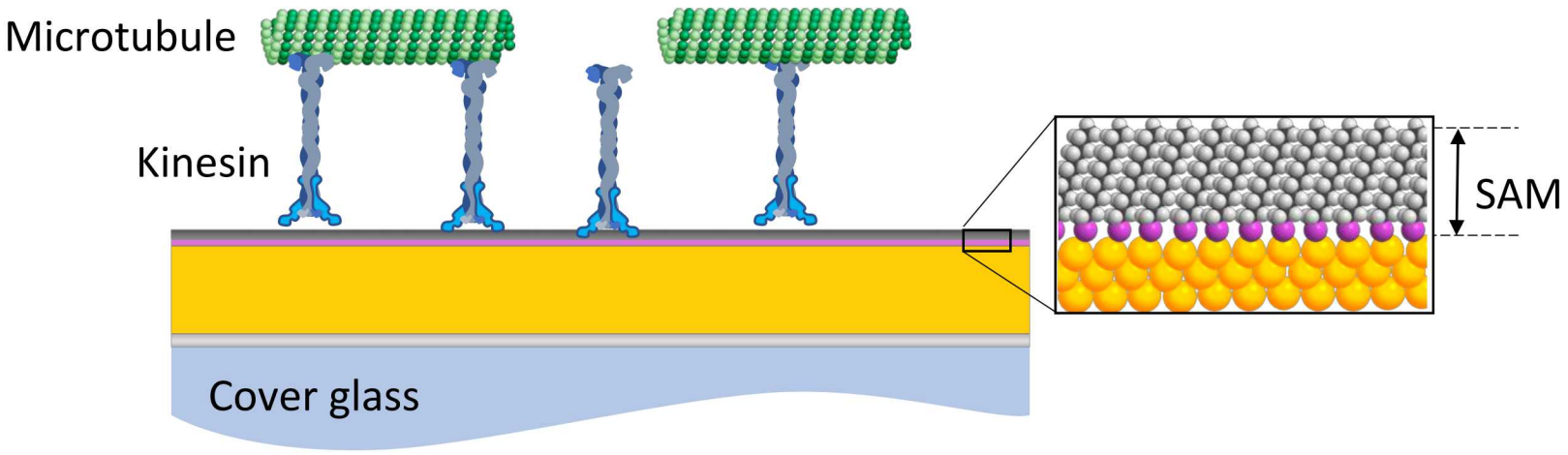
Microtubule
Kinesin
Cover glass
SAM

R=	Functional Group	Characteristics
	CH_3	Neutral & Hydrophobic
	COO^-	Negatively (-) charged @ pH 7.4
	NH_3^+	Positively (+) charged @ pH 7.4

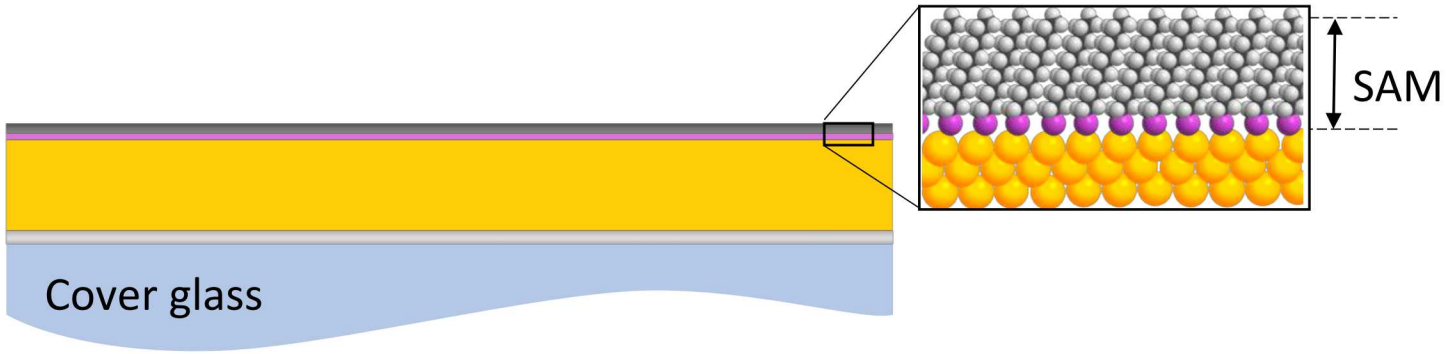

SAMs provide variation in surface charge, however, tend to be smooth on surface

Use SAMs to create nanostructures?

SAMs influence cell attachment and morphology

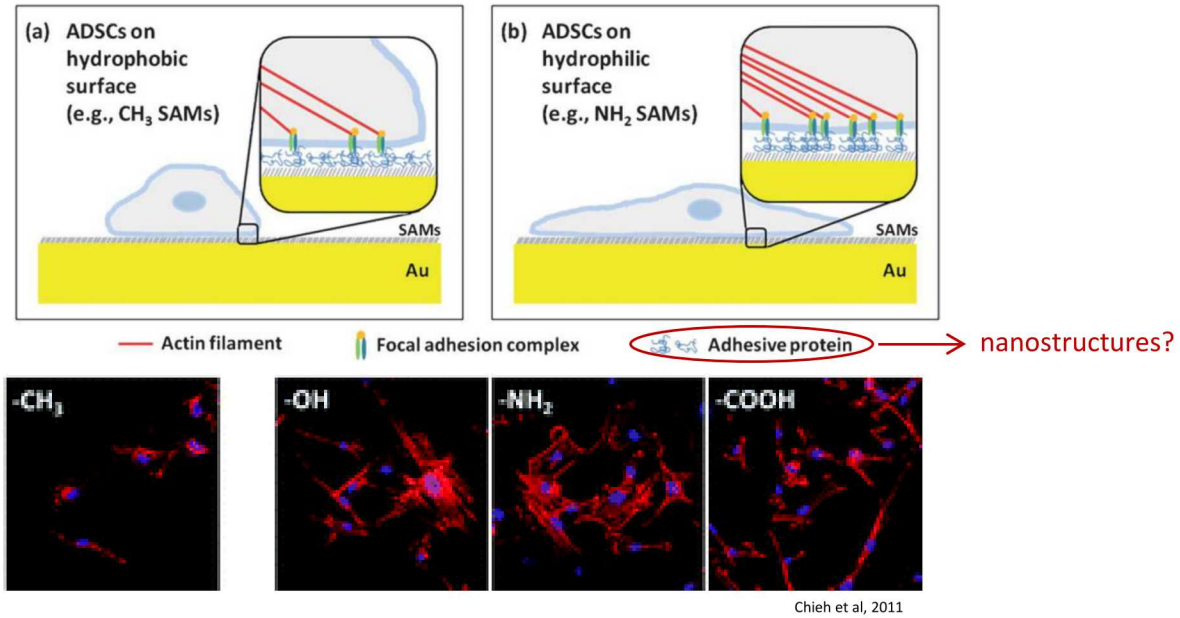

Chieh et al, 2011

- Adhesion of tissue cells to biomaterials is important for tissue engineering
- Response of Adipose derived stromal cells to SAMs was investigated, in which:

SAMs caused surface-induced conformational change in adhesive proteins, further influencing cell attachment and spreading

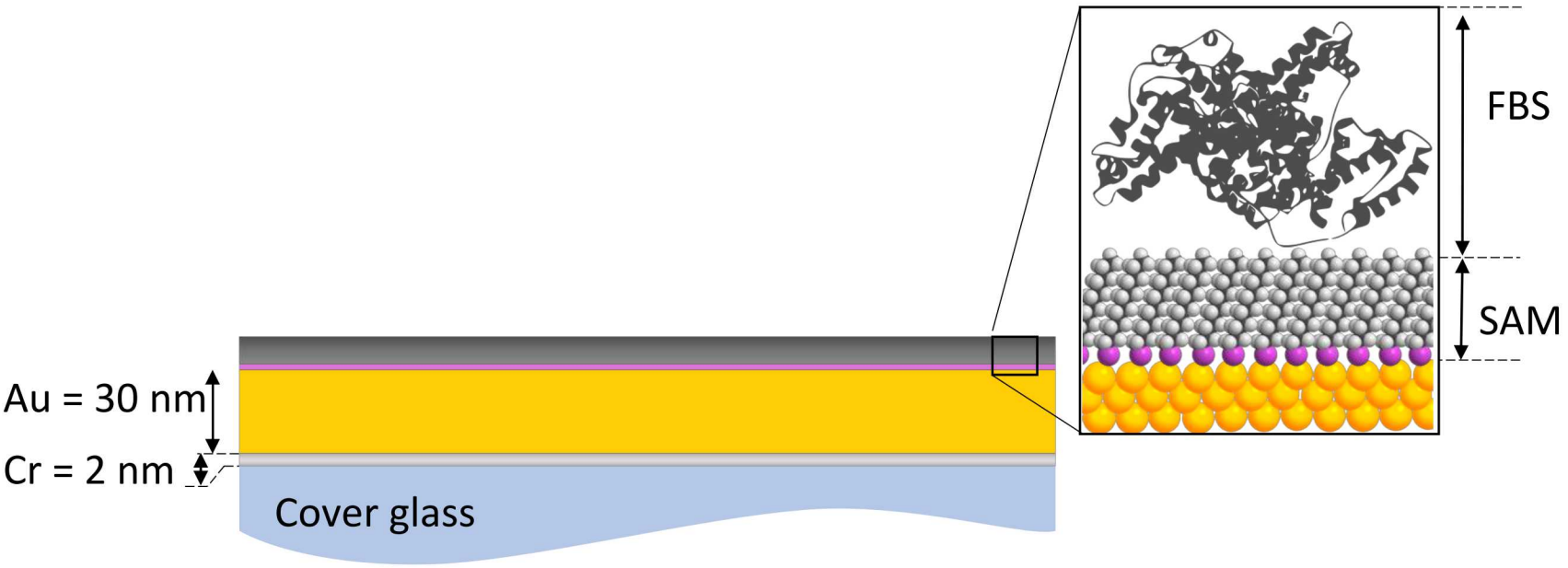

- Fetal bovine serum (FBS) is a supplement for *in vitro* cell culture of eukaryotic cells
  - Mainly contains Bovine Serum albumin (BSA) with various other types of adhesive proteins (fibrinogen and fibronectin)

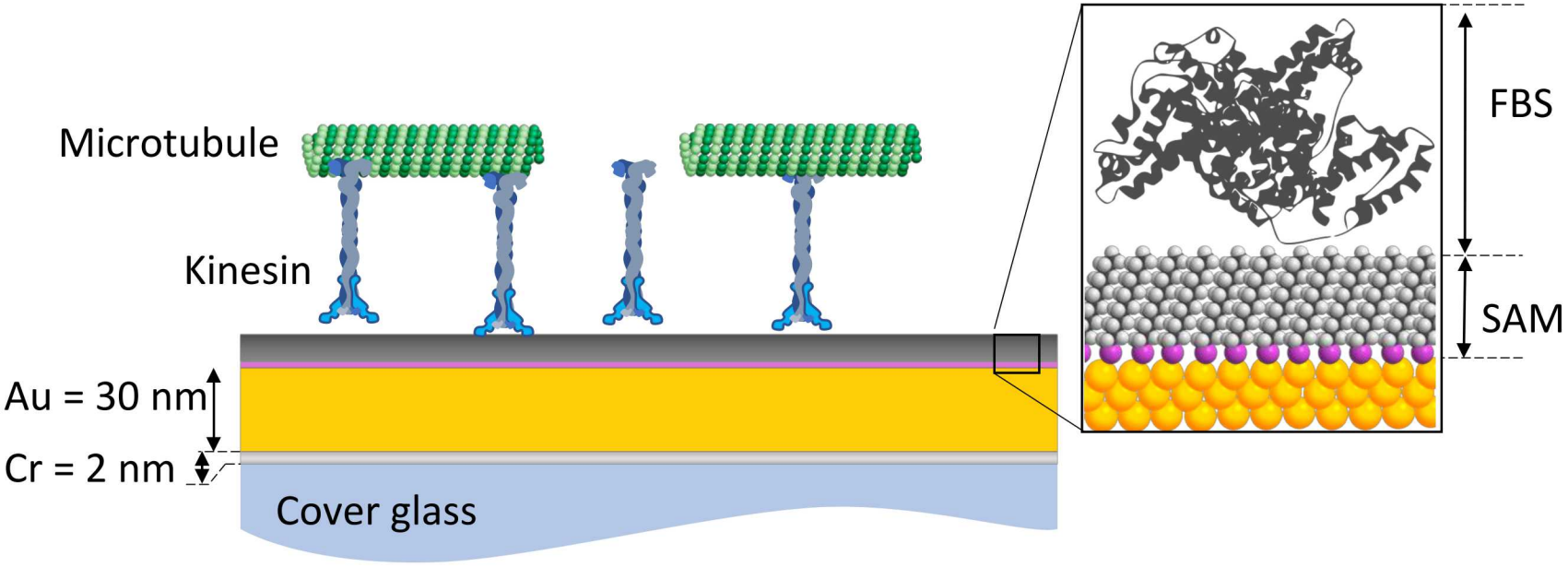
Microtubule
Kinesin
Au = 30 nm
Cr = 2 nm
Cover glass
FBS
SAM

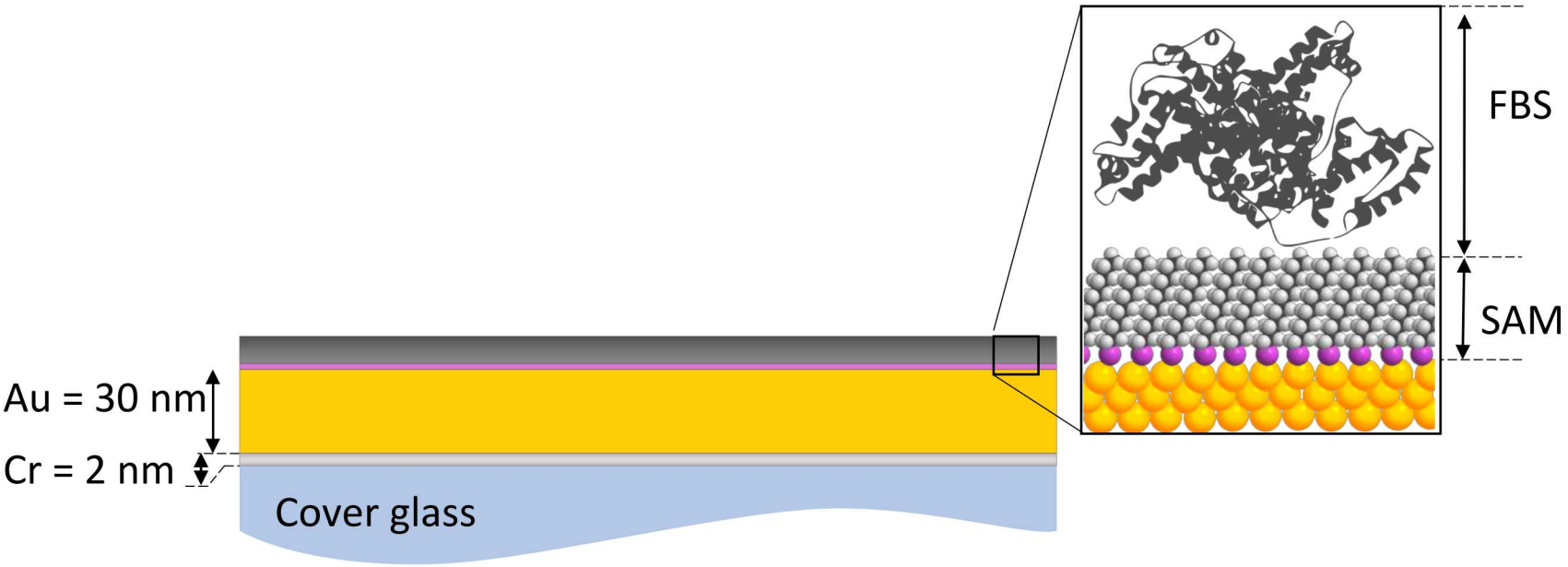

1) SAMs provide variation in surface charge
2) FBS on SAMs provided varying secondary nanostructures

Neutralize and preserve surface?

Silicification of cells

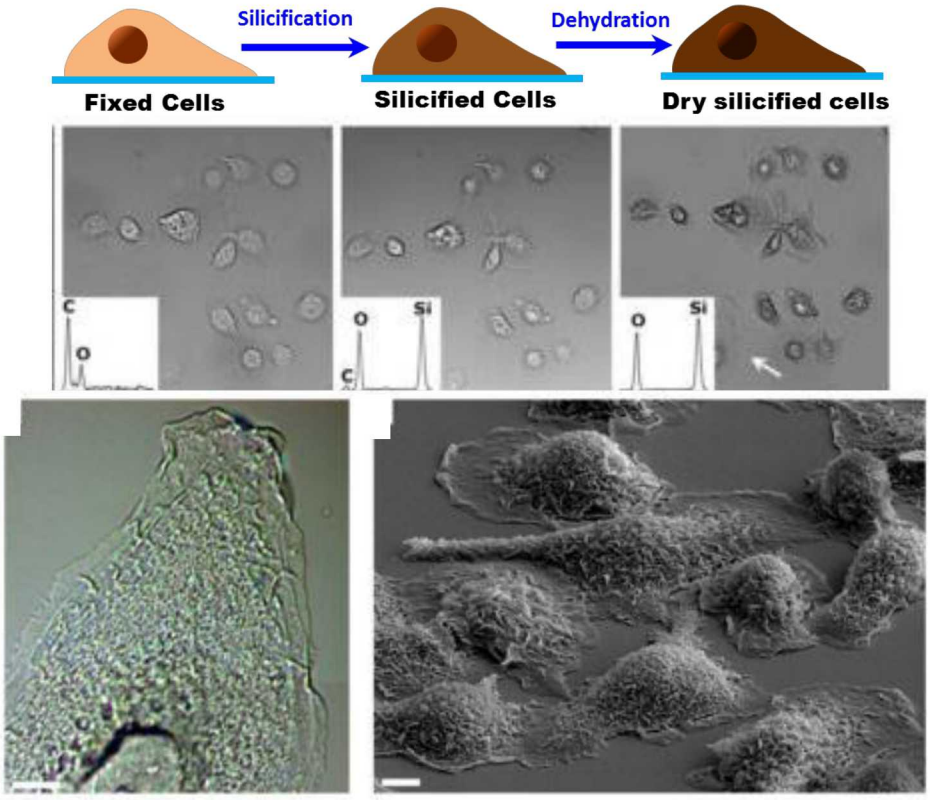

Kaehr et al, 2012

- Size and shape preservation of cellular architectures
- Simple alternative to other common methods of preparation/preservation and can tolerate extreme environments

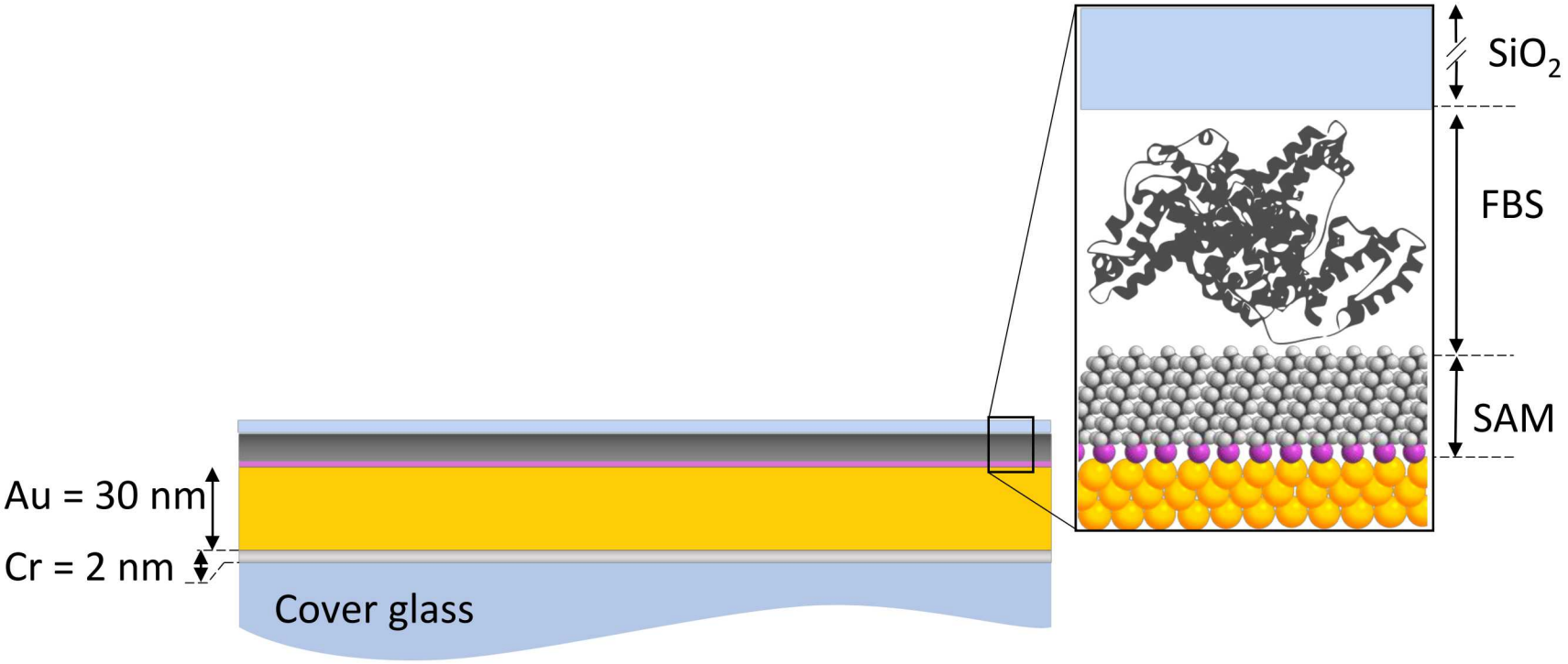

1) Neutralize the surface
2) Preserve structure of underlying layers
3) Provide surface well established for MT motility (i.e., glass) with additional roughness from underlying layers

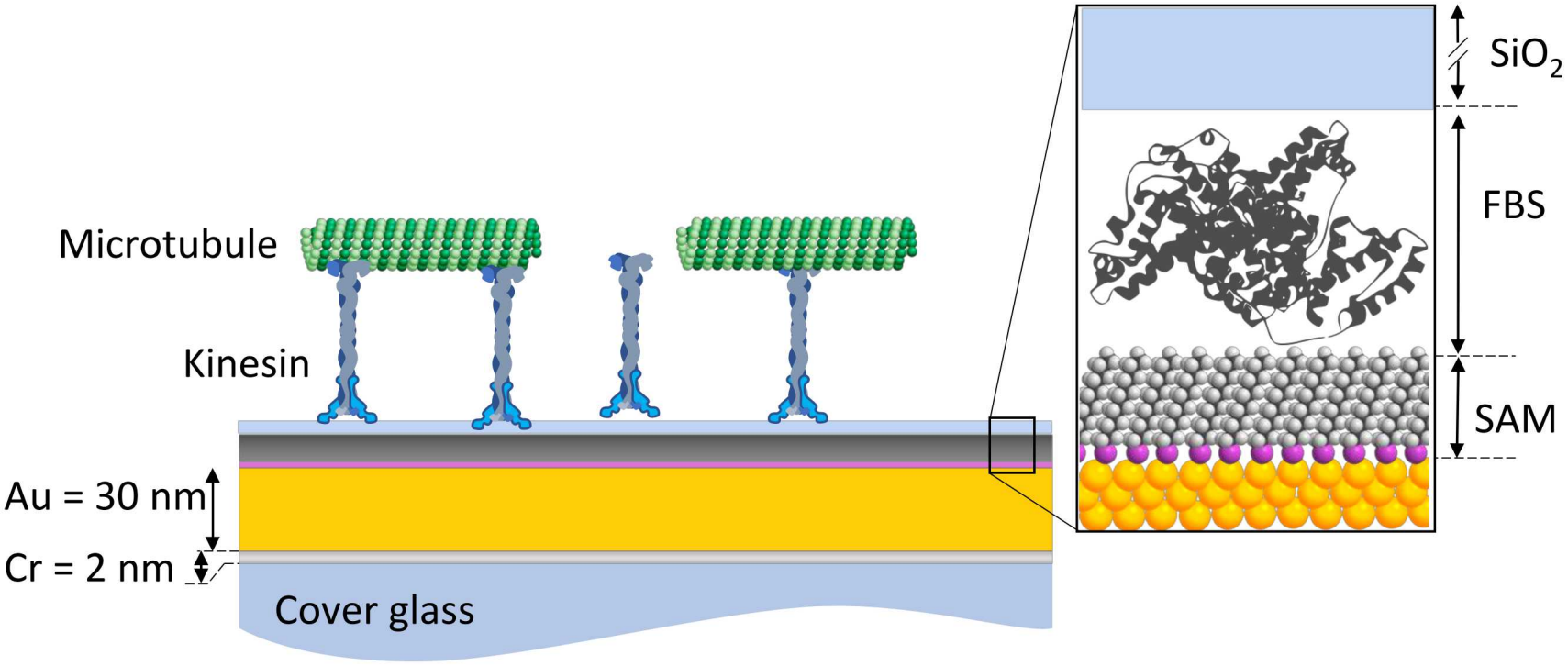
Microtubule
Kinesin
Au = 30 nm
Cr = 2 nm
Cover glass
SiO2
FBS
SAM

Contact Angle Measurements

SAMs

Glass

Au

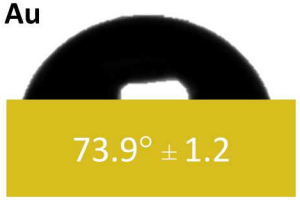

COO^-

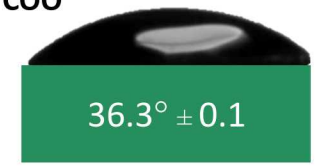

NH_3^+

CH_3

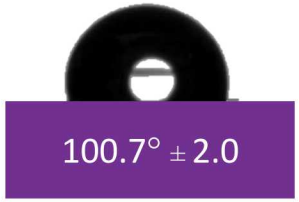

Values= Mean ± SD (n=3)

- Glass, COO^- and NH_3^+ are hydrophilic in nature and increase wettability ($\theta < 90^o$)
- Au was moderately hydrophilic
- CH_3 was hydrophobic ($\theta > 90^o$)

Results in agreement with previously reported values

Contact Angle Measurements

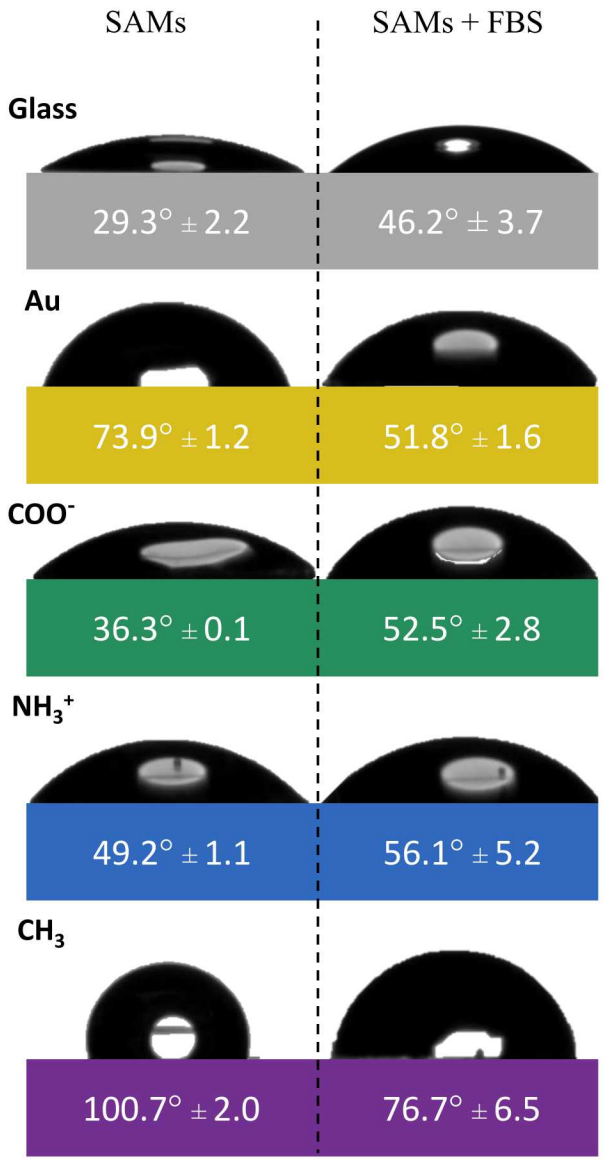

Values= Mean ± SD (n=3)

- Glass, COO^- and NH_3^+ showed an increase in θ
- Au and CH3 showed a decrease in θ
- Overall, all surfaces were moderately hydrophilic

Results in agreement with previously reported reduction in θ for hydrophobic surfaces, and increase in θ for hydrophilic surfaces due to incubation in FBS

Contact Angle Measurements

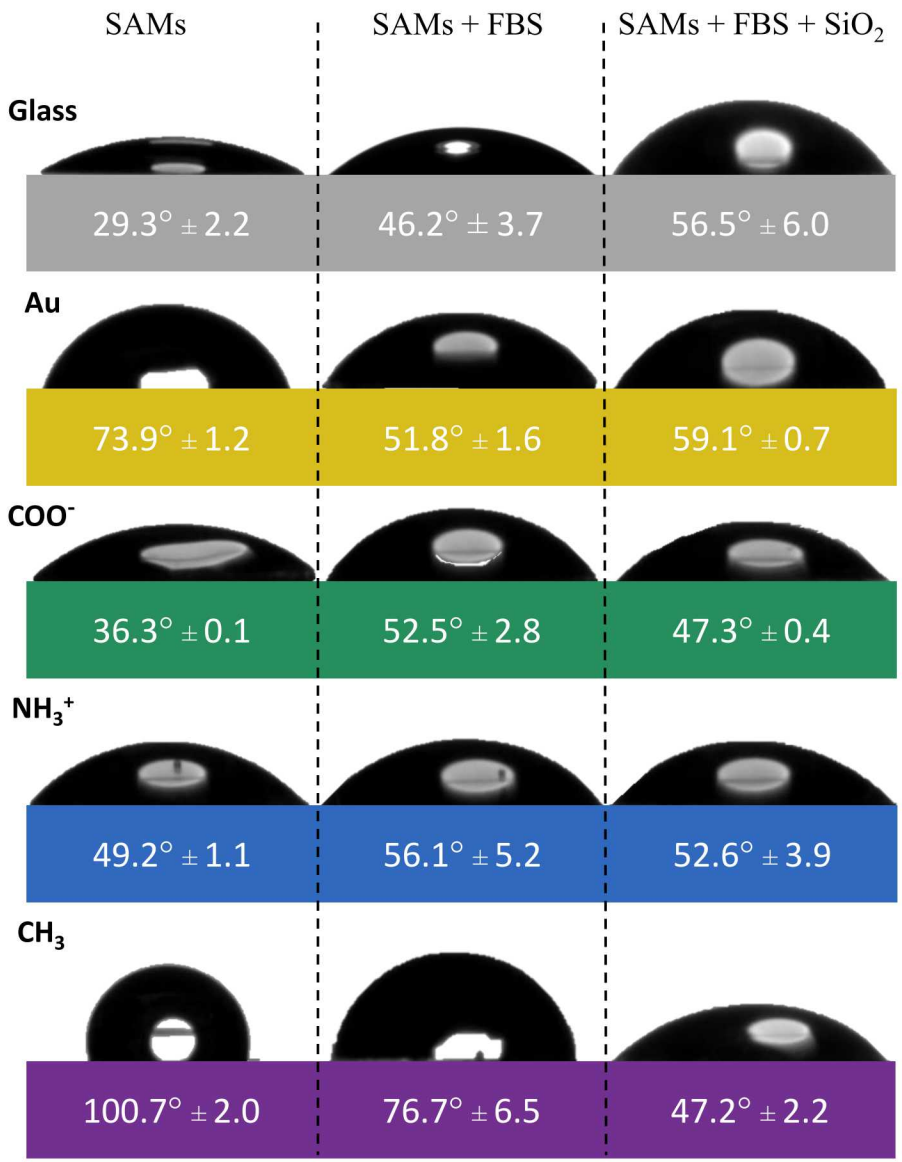

Values= Mean ± SD (n=3)

- θ was moderately hydrophilic and similar to previous layer
- CH_3 most affected by wettability with greatest decrease in θ

Results support SiO_2 outermost layer

X-ray photoelectron spectroscopy (XPS) of SAMs

Substrate	Atomic composition (%)				
	Au(4f)	C(1s)	N(1s)	O(1s)	Si(2s)
Glass	0(0)	14.6 (0)	1.0 (0)	60.7 (72.1)	21.7 (26.2)
Glass+ BSA	0	47.0	10.0	32.0	9.0
Glass+ BSA+ Si	0	35.9	2.4	44.2	16.6
Au	71.6 (100)	25.9 (0)	0 (0)	1.7 (0)	0.6 (0)
Au + BSA	28.8	47.9	1.03	12.0	0.5
Au + BSA + Si	11.1	37.4	4.1	37.3	8.8
CH_3	61.3(53.8)	37.8 (46.1)	0 (0)	0 (0)	0.8 (0)
CH_3 + BSA	23.3	53.9	7.8	10.5	4.0
CH_3 + BSA + Si	10.3	36.7	3.1	36.4	13.3
COO^-	57.6 (51.8)	36.1 (40.7)	0 (0)	5.5 (7.4)	0 (0)
COO^- + BSA	29.5	51.0	8.1	11.1	0.03
COO^- + BSA + Si	11.8	36.2	1.3	37.2	11.9
NH_3^+	40.0 (53.8)	51.3 (42.3)	1.8 (3.85)	4.0 (0)	1.2 (0)
NH_3^+ + BSA	28.1	52.3	8.2	10.1	0.7
NH_3^+ + BSA + Si	10.2	36.0	2.1	38.6	12.0

XPS results were in agreement with expected theoretical values (shown in parenthesis)

- All SAMs had Au and carbon (alkane chain)
- COO^- and NH_3^+ confirmed by presence of oxygen and nitrogen

XPS of FBS coated SAMs

Substrate	Atomic composition (%)				
	Au(4f)	C(1s)	N(1s)	O(1s)	Si(2s)
Glass	0(0)	14.6 (0)	1.0 (0)	60.7 (72.1)	21.7 (26.2)
Glass+ BSA	0	47.0	10.0	32.0	9.0
Glass+ BSA+ Si	0	35.9	2.4	44.2	16.6
Au	71.6 (100)	25.9 (0)	0 (0)	1.7 (0)	0.6 (0)
Au + BSA	28.8	47.9	1.03	12.0	0.5
Au + BSA + Si	11.1	37.4	4.1	37.3	8.8
CH_3	61.3(53.8)	37.8 (46.1)	0 (0)	0 (0)	0.8 (0)
CH_3 + BSA	23.3	53.9	7.8	10.5	4.0
CH_3 + BSA + Si	10.3	36.7	3.1	36.4	13.3
COO^-	57.6 (51.8)	36.1 (40.7)	0 (0)	5.5 (7.4)	0 (0)
COO^- + BSA	29.5	51.0	8.1	11.1	0.03
COO^- + BSA + Si	11.8	36.2	1.3	37.2	11.9
NH_3^+	40.0 (53.8)	51.3 (42.3)	1.8 (3.85)	4.0 (0)	1.2 (0)
NH_3^+ + BSA	28.1	52.3	8.2	10.1	0.7
NH_3^+ + BSA + Si	10.2	36.0	2.1	38.6	12.0

- Increase in carbon, nitrogen and oxygen at % (from amine and carboxyl groups in proteins)
- Au decreased due to layer of protein

XPS of silicified FBS coated SAMs

Substrate	Atomic composition (%)				
	Au(4f)	C(1s)	N(1s)	O(1s)	Si(2s)
Glass	0(0)	14.6 (0)	1.0 (0)	60.7 (72.1)	21.7 (26.2)
Glass+ BSA	0	47.0	10.0	32.0	9.0
Glass+ BSA+ Si	0	35.9	2.4	44.2	16.6
Au	71.6 (100)	25.9 (0)	0 (0)	1.7 (0)	0.6 (0)
Au + BSA	28.8	47.9	1.03	12.0	0.5
Au + BSA + Si	11.1	37.4	4.1	37.3	8.8
CH_3	61.3(53.8)	37.8 (46.1)	0 (0)	0 (0)	0.8 (0)
CH_3 + BSA	23.3	53.9	7.8	10.5	4.0
CH_3 + BSA + Si	10.3	36.7	3.1	36.4	13.3
COO^-	57.6 (51.8)	36.1 (40.7)	0 (0)	5.5 (7.4)	0 (0)
COO^- + BSA	29.5	51.0	8.1	11.1	0.03
COO^- + BSA + Si	11.8	36.2	1.3	37.2	11.9
NH_3^+	40.0 (53.8)	51.3 (42.3)	1.8 (3.85)	4.0 (0)	1.2 (0)
NH_3^+ + BSA	28.1	52.3	8.2	10.1	0.7
NH_3^+ + BSA + Si	10.2	36.0	2.1	38.6	12.0

- Silicon and oxygen at. % increased due to silicification process
- Au, carbon and nitrogen at. % decreased

Topography and roughness of SAMs

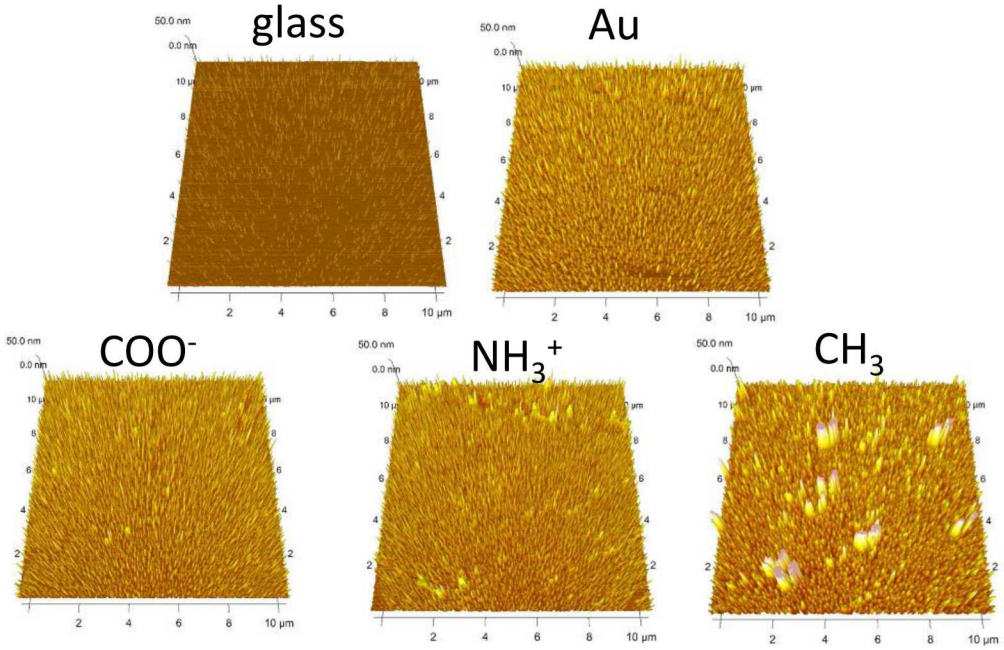

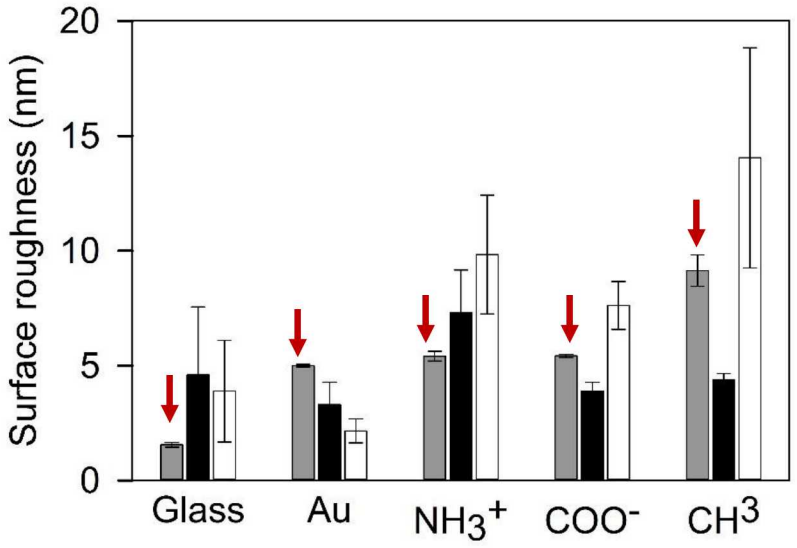

- Surface roughness of Au is high possibly due to defects during deposition process
- CH_3 had the roughest surface (tall peaks) of all SAMs
  - Desorption exposed underlying Au layer

Topography and roughness of FBS coated SAMs

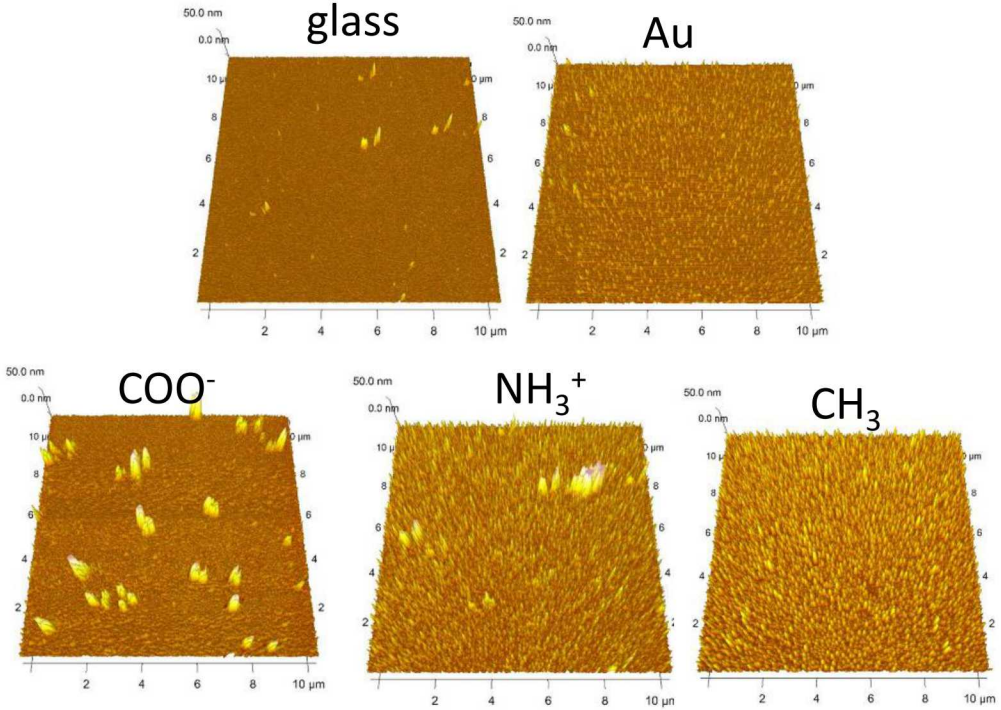

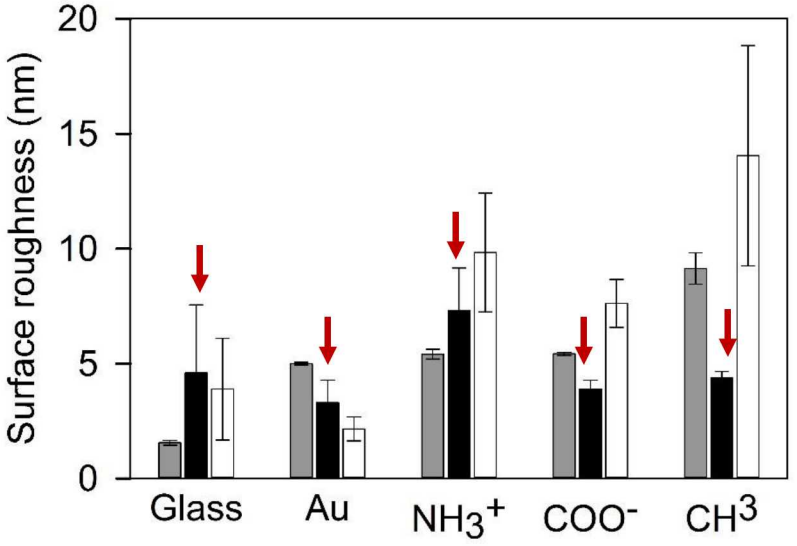

- NH_3^+ had highest average roughness
- Glass and NH_3^+ (both hydrophilic) increased in roughness compared to previous (SAMs) layer
- COO^- (hydrophilic) roughness decreased compared to previous SAM layer, similar to Au and CH_3 (both hydrophobic)

Topography and roughness of silicified FBS coated SAMs

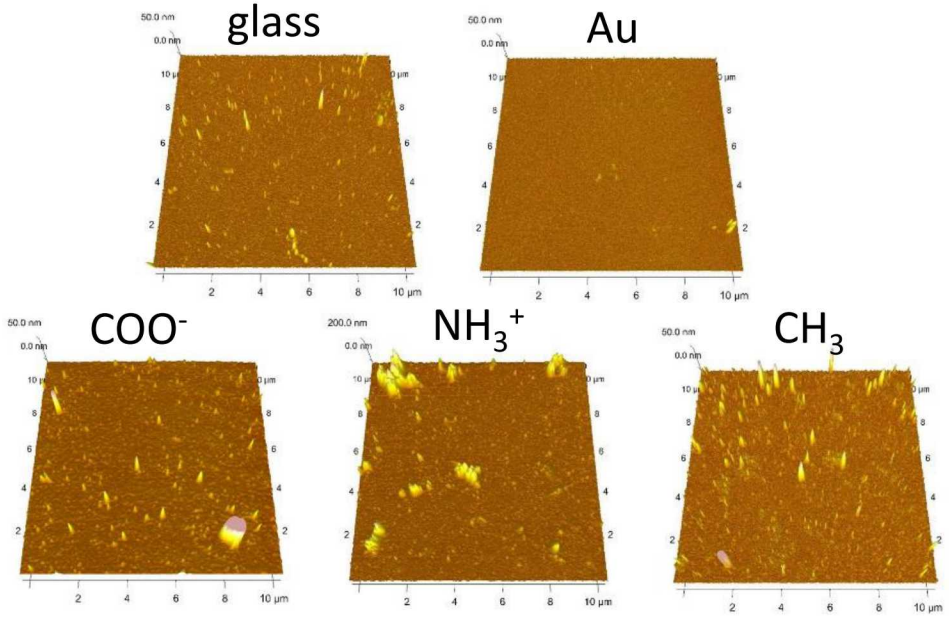

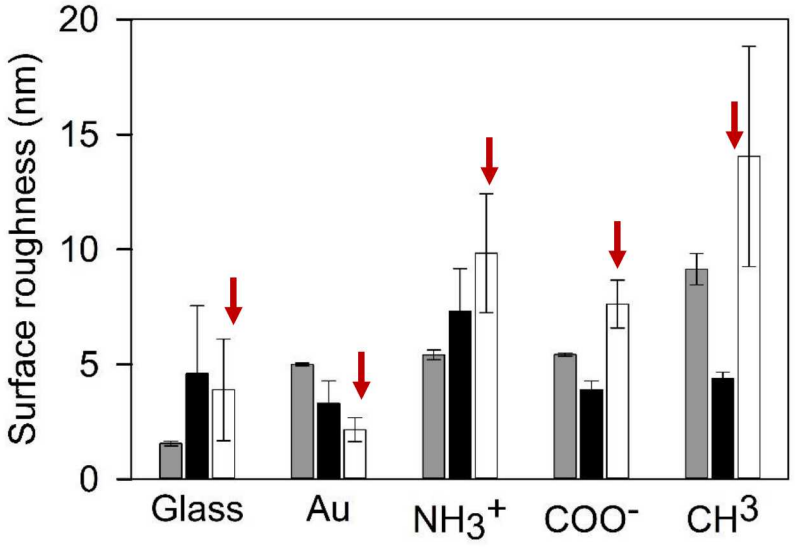

- All three surfaces with underlying SAMs had higher average roughness values compared to controls (glass and Au)
- Controls roughness decreased compared to previous FBS layer, indicating silicification smoothed out surfaces that lack SAMs first layer
- Silicified CH_3 had highest average roughness compared to silicified surfaces and remaining layers

MT Tracking

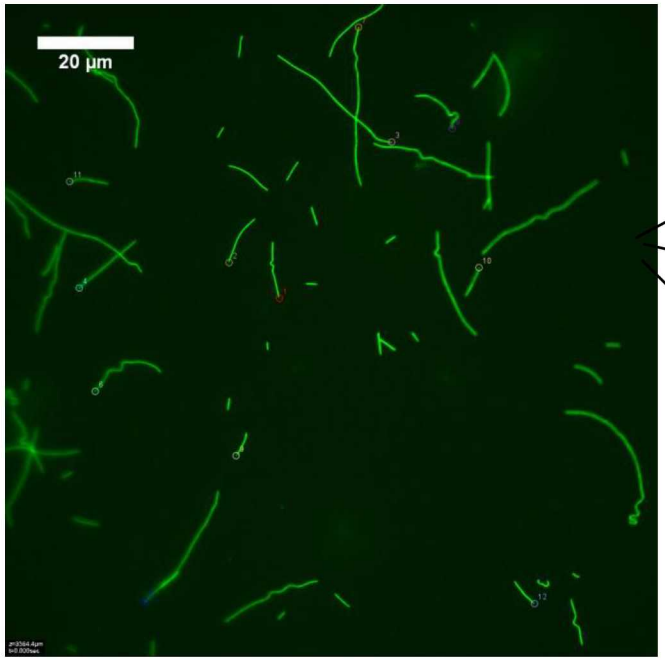

Velocity

Trajectory

displacement

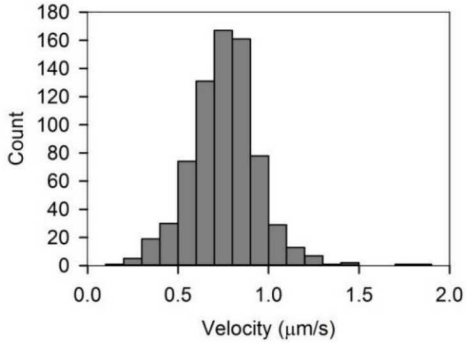

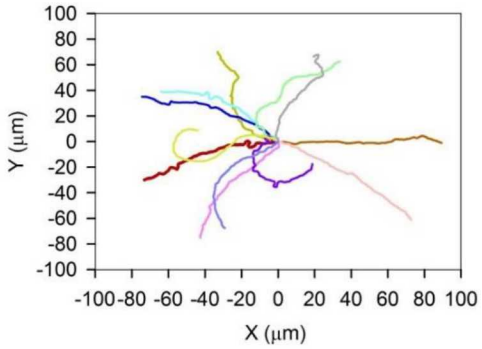

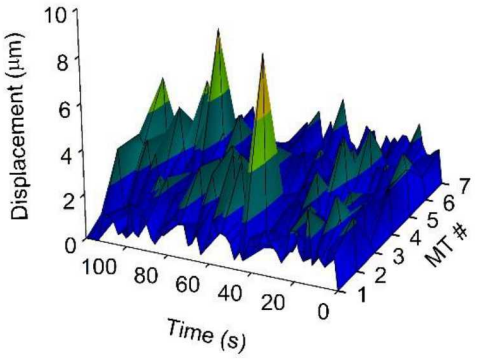

Frame-to-frame tracking of MTs to evaluate changes in MT movement and speed on the different surfaces

MT velocity on SAMs

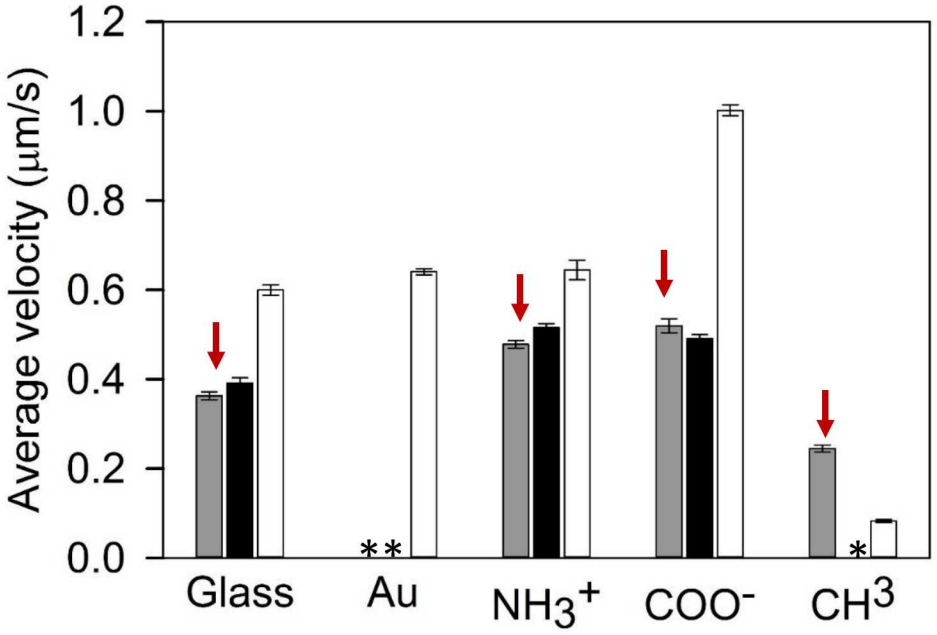

- NH_3^+ and COO^- had similar average velocity (similar roughness)
- CH_3^+ showed lowest average velocity (roughest surface)

Surface topography/roughness effected MT velocity

MT velocity on FBS coated SAMs

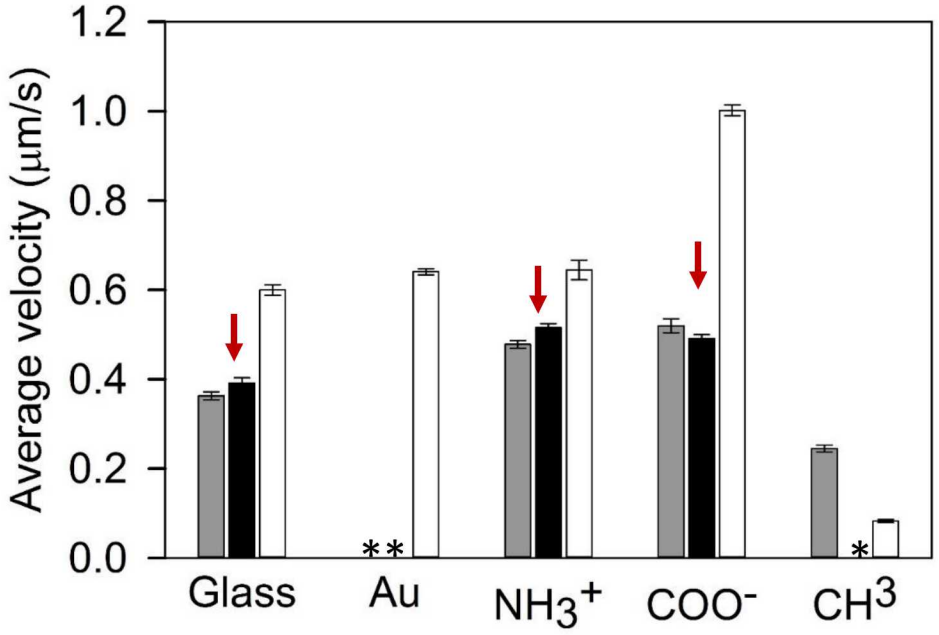

- MT transport only on hydrophilic underlying SAMs surfaces
- NH_3^+ had highest average velocity (roughest surface)
- Velocity of MTs on FBS coated SAMs did not show significant difference compared to previous SAMs layer

Protein adsorption and degree of denaturation influenced velocity

MT velocity on silicified FBS coated SAMs

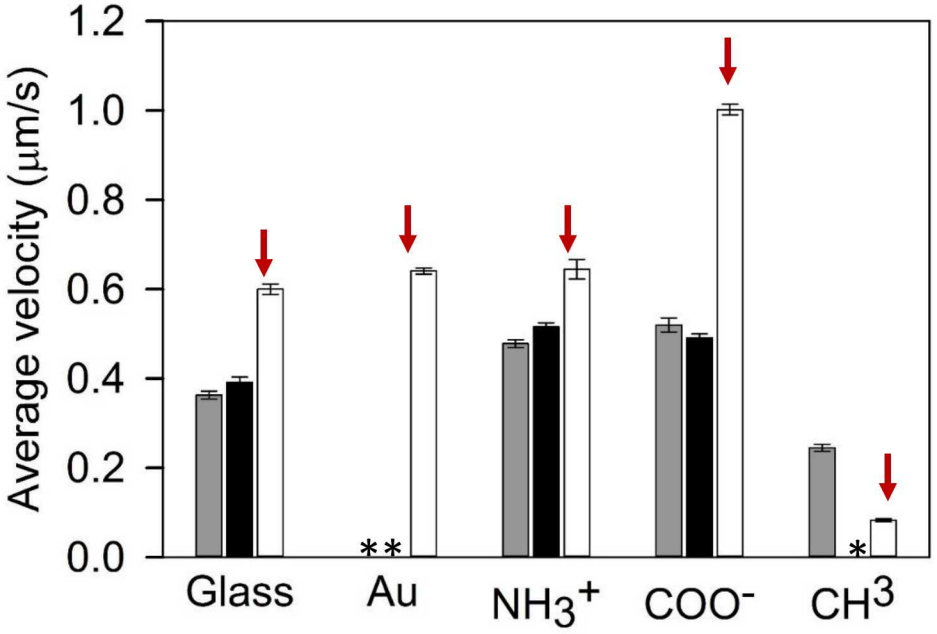

- Silicification of substrates enabled kinesin attachment and MT motility on all SAMs surfaces
- Highest average velocity compared to the two previous layers (except for CH3)
- CH_3 lowest average velocity (highest roughness among silicified surfaces, and compared to the rest of the SAMs from previous two layers)
- Average MT velocity on COO^- almost doubled compared to previous two layers

Silicification enabled faster MT transport, independent of surface topography/roughness on most substrates

MT displacement and trajectories on SAMs

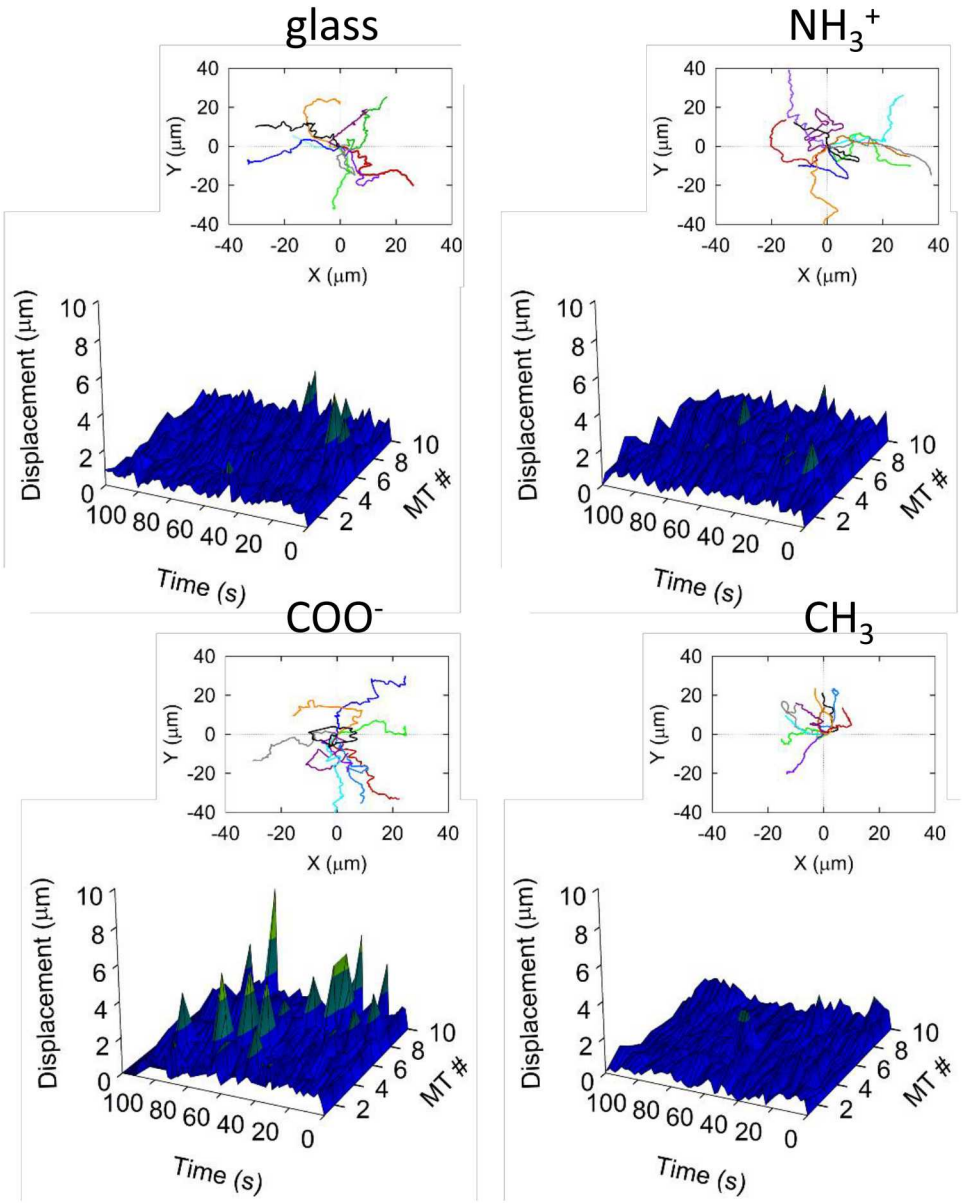

- Glass and NH_3^+ showed "random walk" with random and consistent displacement
- COO^- highest MT displacement
- CH_3^+ minimal movement with constant displacement (roughest surface)

Surface topography/roughness influenced MT transport

MT displacement and trajectories on FBS coated SAMs

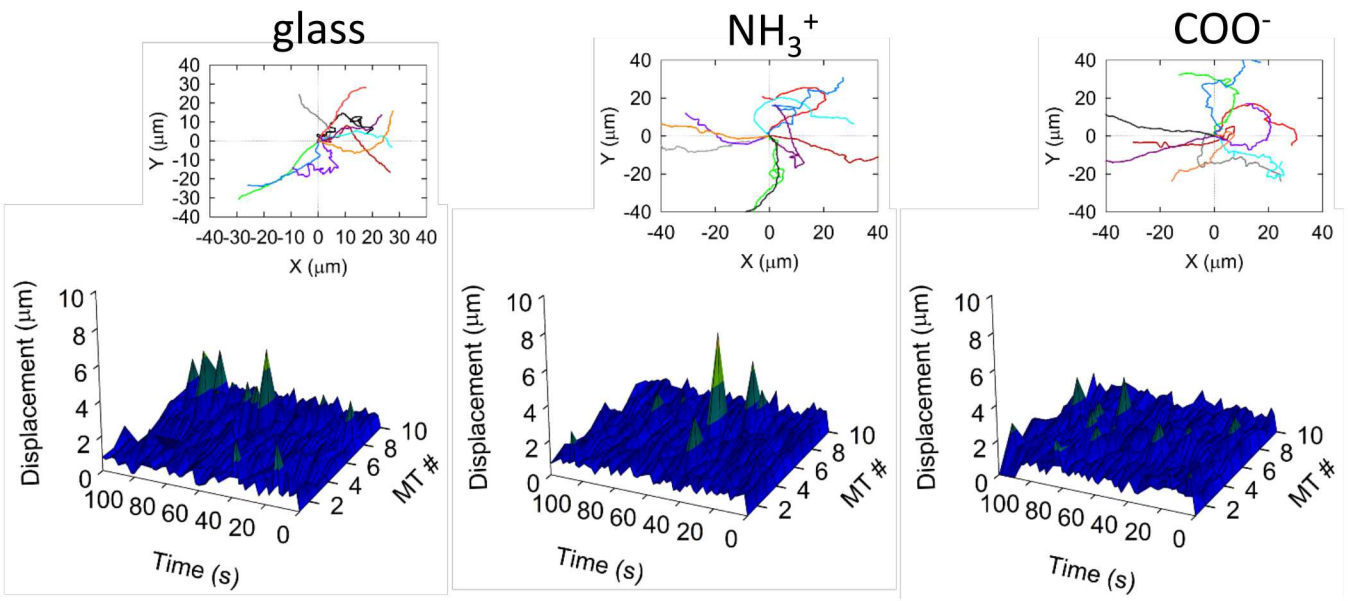

- NH3+ showed smoother gliding behavior with a subtle increase in displacement compared to previous layer
- COO- showed smoother gliding behavior and consistent displacement compared to previous layer

FBS did not promote adhesion of kinesin motors with only three of the surfaces promoted MT motility, but overall allowed for smooth MT gliding

MT displacement and trajectories on silicified FBS coated SAMs

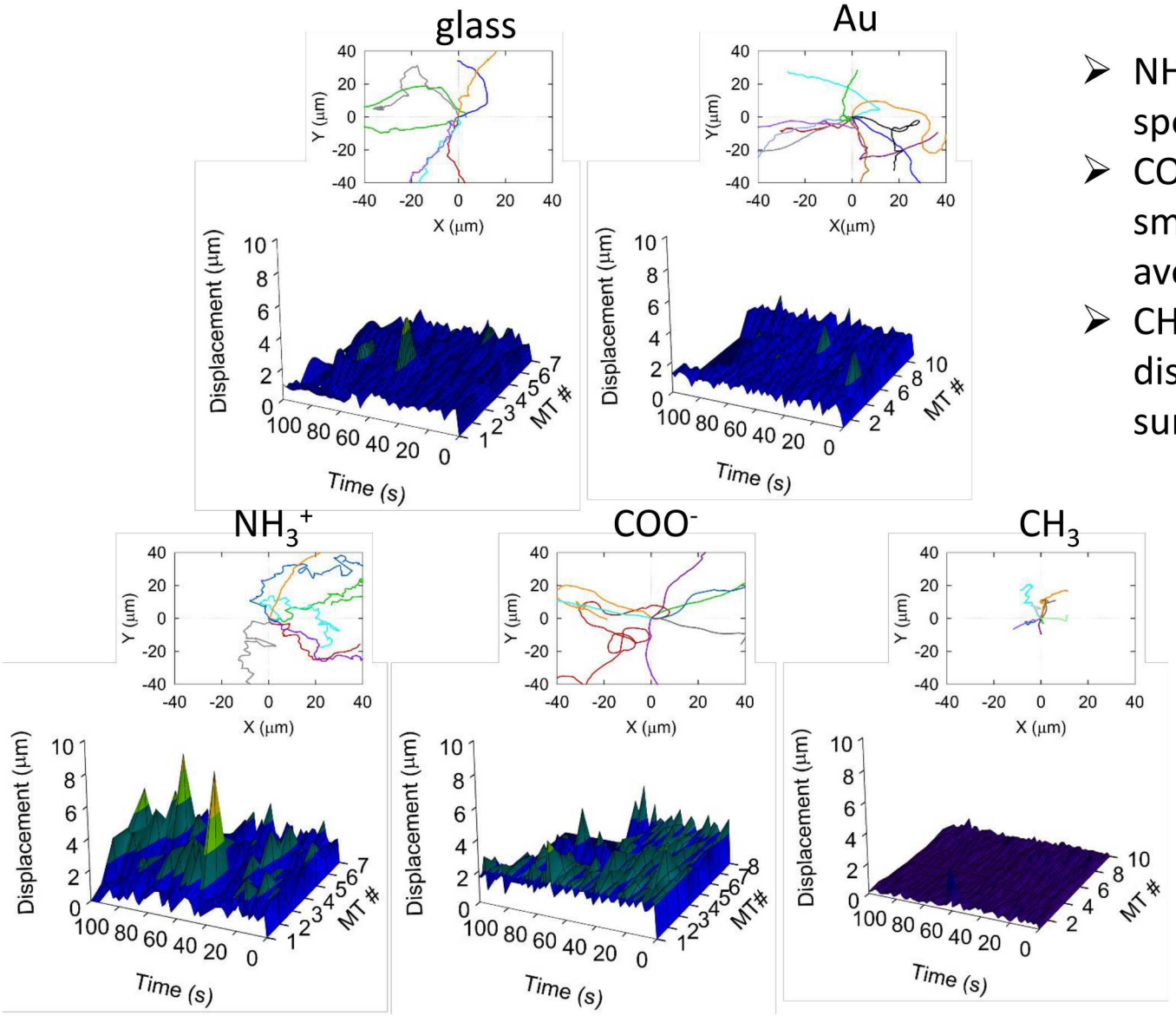

- NH_3^+ showed high and sporadic displacement
- COO^- trajectories were smooth with highest average displacement
- CH_3 showed minimal displacement (roughest surface)

Silicification allowed for MT transport on all surfaces with higher average displacement (except for CH_3)

Conclusions

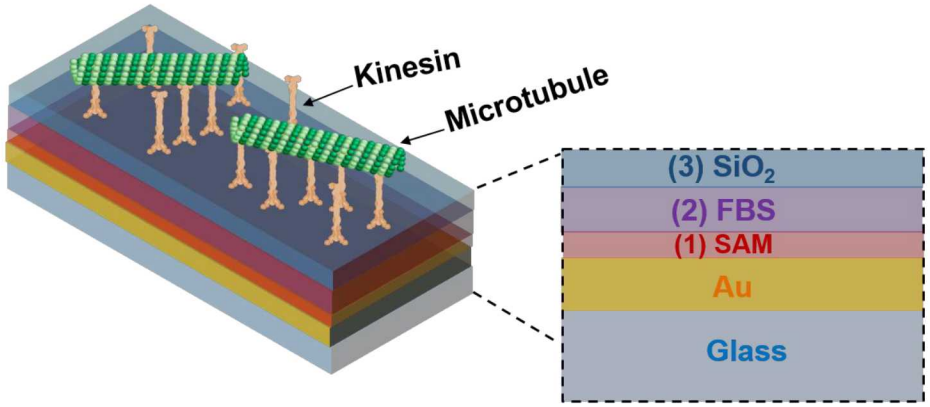

- MT transport behaviors were evaluated on three layers of biocompatible substrates: SAMs, Protein (FBS) coated SAMs, and Silicified protein coated SAMs
- Each layer was characterized by various methods to determine composition and roughness of substrates including XPS, water contact angle, and AFM
- COO^- terminated SAMs was most reliable for motor adhesion and MT transport (all three layers)
- CH_3 terminated SAMs impeded MT movement (roughest surface)
- FBS (2^{nd}) layer had least kinesin attachment, while silicified (3^{rd}) layer supported kinesin attachment and MT transport on all surfaces

Research outcomes

- Investigated the affect of defective building blocks on the active assembly and behavior of motor-driven MT spools
  - Identified quality control mechanisms employed by spools through preferential release of defective MT domains over time
- Established biocompatible substrates to investigate the effects of surface chemistry and roughness on MT transport
  - Identified factors that influence MT transport by characterizing each substrate
  - Determined substrate compatibility with MT transport by characterizing MT velocity, trajectories and displacement

Future directions

Segmented spools:

- In depth characterization of time- dependent release of defective non-bonding MTs from spools (microfluidic device)
- Characterization of spools using high resolution techniques (SEM and AFM) to:
  - determine differences in structures based on non-bonding MT levels
  - reveal shearing sites of non-bonding MTs within spools

Kinesin-MT transport:

- Identify layer thicknesses to determine if layers integrated (e.g. using SPR)
- Study transport on more complex substrates:
  - Microcontact printing to attach different SAMs on same substrate
  - 3-D complex structures (e.g. silicified cells)

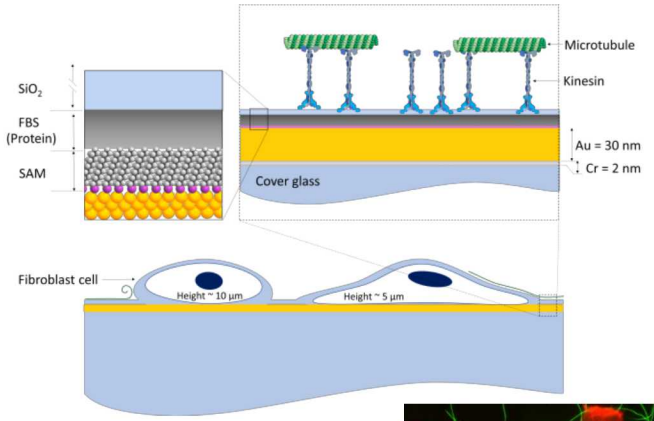

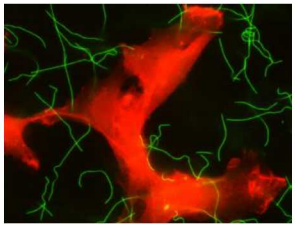

Acknowledgments

Dr. George D. Bachand
Dr. Andrew P. Shreve
Dr. Virginia VanDelinder
Dr. Zachary Imam
Dr. Erik D. Spoerke
Dr. Nicholas J.D. Martinez
Jimin Guo
Victoria Lujan
Ian Sickafoose
Jessica Depoy
Michael T. Brumbach
Dr. C. Jeffery Brinker
Dr. Jaquelin Weeks
Dr. Brad Jones
Dr. Sergei Ivanov
Dr. Nick J. Carroll
Dr. Francesca Cavallo

This work was supported by the U.S. Department of Energy, Office of Basic Energy Sciences, Division of Materials Sciences and Engineering (BES-MSE). This work was performed, in part, at the Center for Integrated Nanotechnologies, an Office of Science User Facility operated for the U.S. Department of Energy (DOE) Office of Science (User Project 2017AU0006; PI: Martinez). Sandia National Laboratories is a multi-mission laboratory managed and operated by National Technology and Engineering Solutions of Sandia, LLC., a wholly owned subsidiary of Honeywell International, Inc., for the U.S. DOE's National Nuclear Security Administration under contract DE-NA-0003525.

Questions?

Motor proteins and filaments *in vivo*

Cytoskeletal filaments and motor proteins are central to many biological processes

https://en.wikipedia.org/wiki/Spindle_apparatus

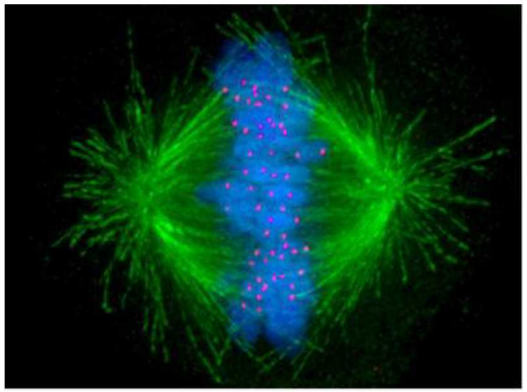

Splitting chromosomes (mitosis and meiosis)

https://biodifferences.com/difference-between-cilia-and-flagella.html

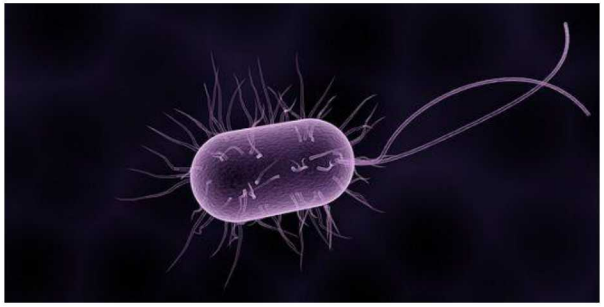

Cilia and flagella (motility)

https://www.thoughtco.com/neurons-373486

Vesicular trafficking

Contact Angle

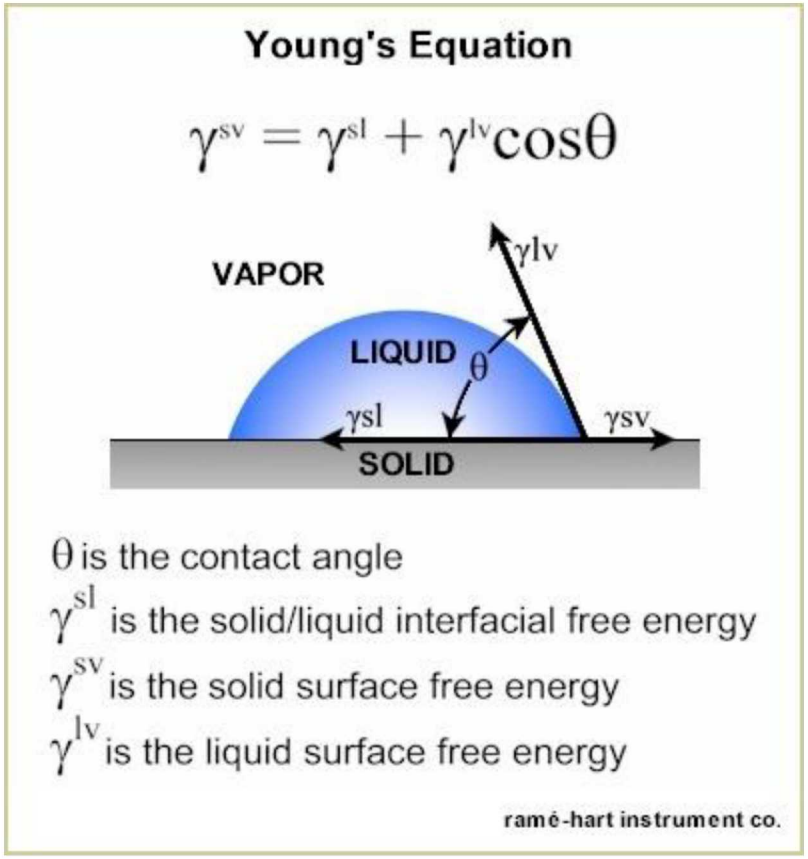

Angle formed by the liquid-gas interface with respect to the solid

>90° = hydrophobic

< 90°= hydrophilic

X-ray photoelectron spectroscopy (XPS)

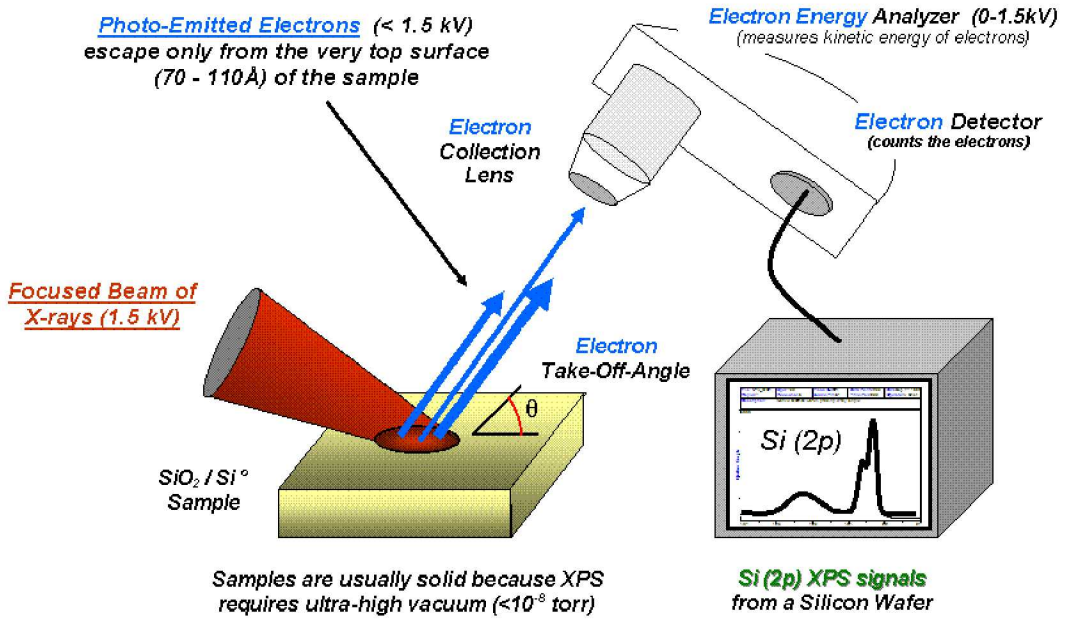

- Surface sensitive technique that measure elemental composition of material
- Irradiate material with a beam of x-rays and measure kinetic energy (top 10 nm)

Atomic Force Microscopy (AFM)

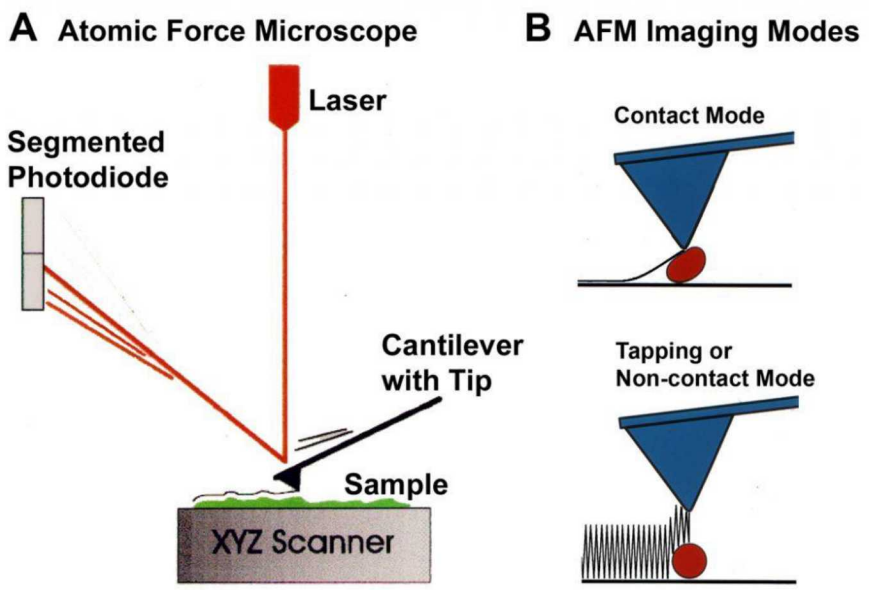

A scanning probe technique in which a sharp tip at end of cantilever scans surface, and tip-surface interaction maps topography of surface

Average length and count of bonding and non-bonding MT domains in segmented MTs

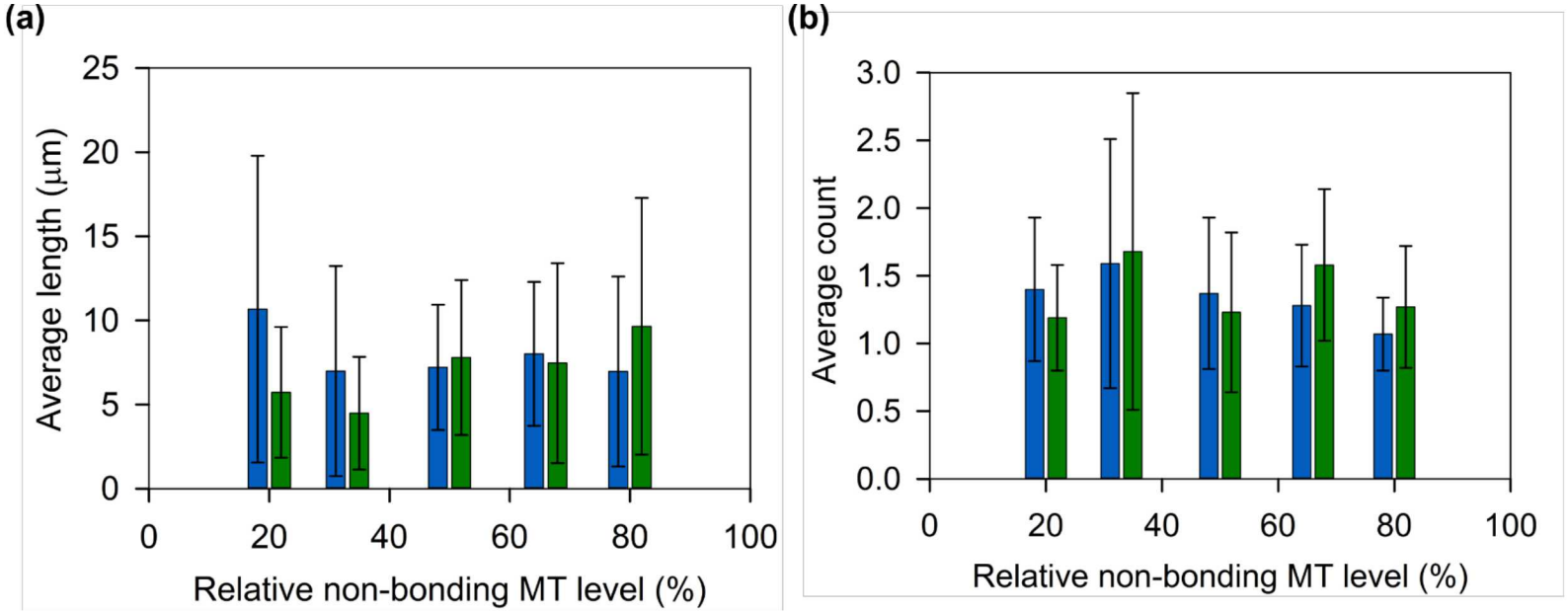

Blue bars = bonding
Green bonds= non-bonding

Average density and length of unattached non-bonding MTs

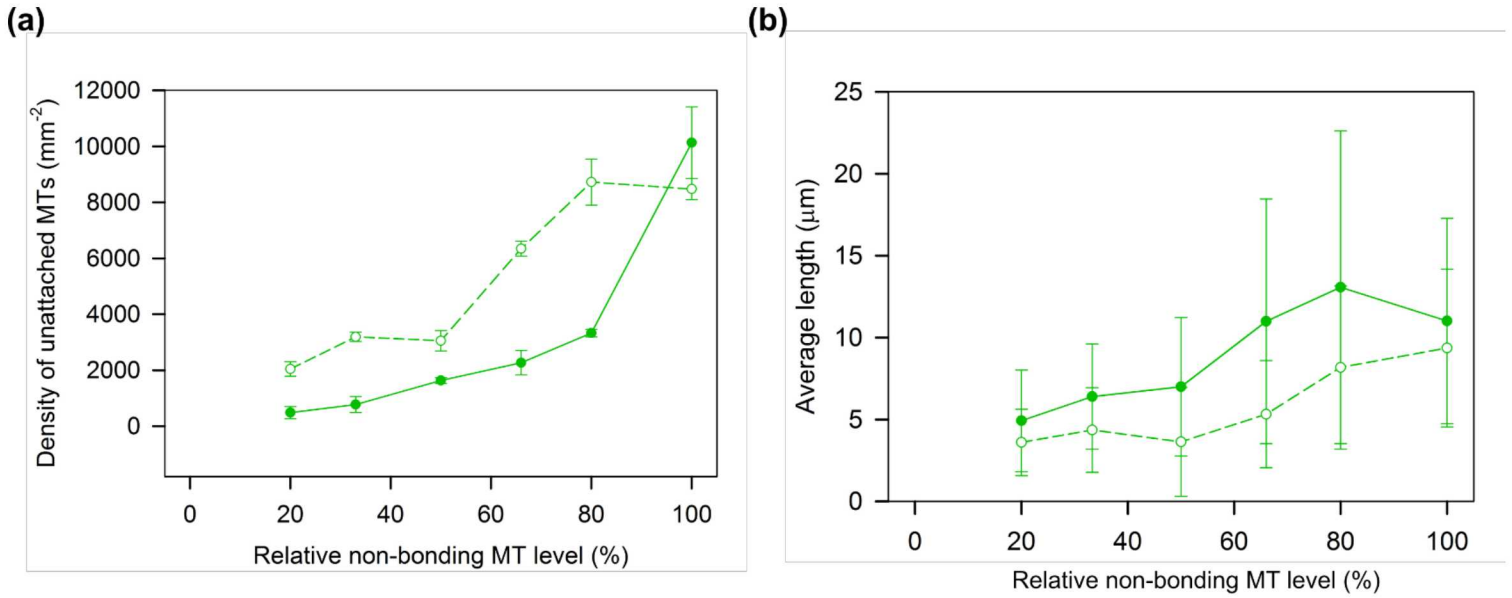

Solid line/closed circles= prior to adding Qds (t=0)
Dashed lines/open circles= after adding Qds (t= 30min)

Average change in density and length of bonding MTs

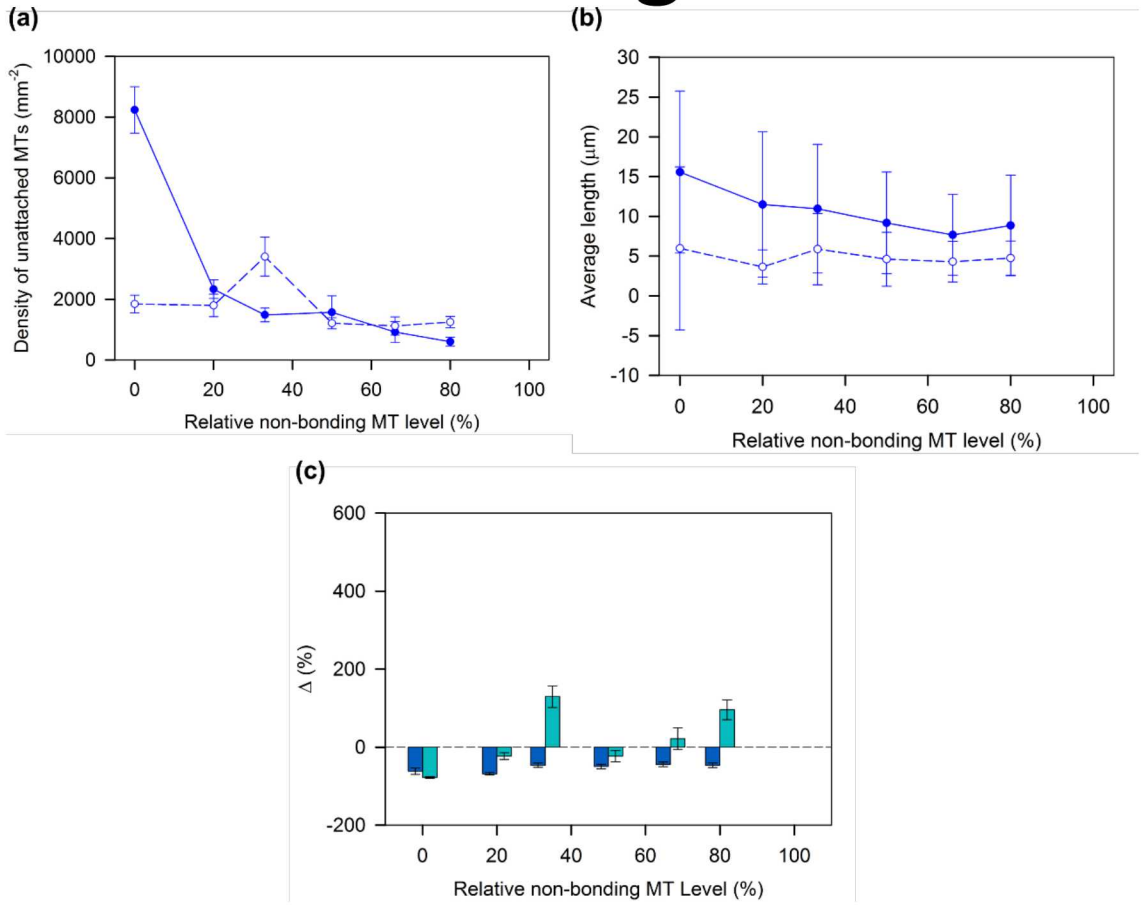

Solid line/closed circles= prior to adding Qds (t=0)
Dashed lines/open circles= after adding Qds (t= 30min)
Light blue bars= change in average density
Dark blue bars= change in average count

Average change in density and length of segmented MTs

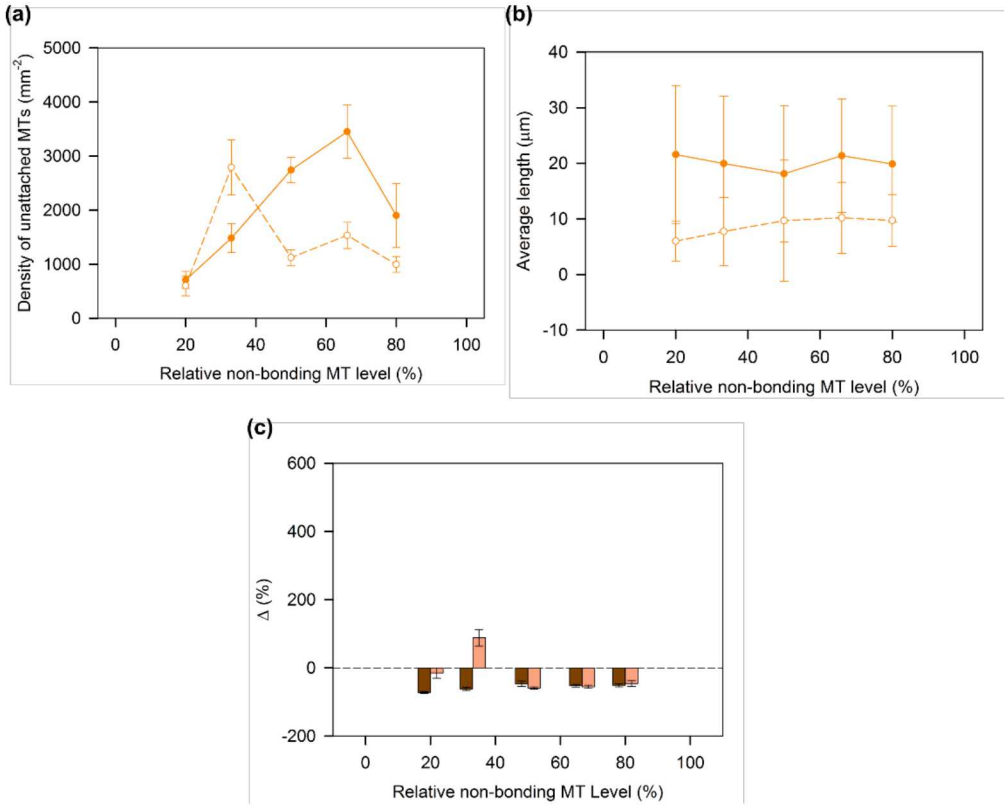

Solid line/closed circles= prior to adding Qds (t=0)
Dashed lines/open circles= after adding Qds (t= 30min)
Light orange= change in average density
Brown bars= change in average count

Thickness of spools

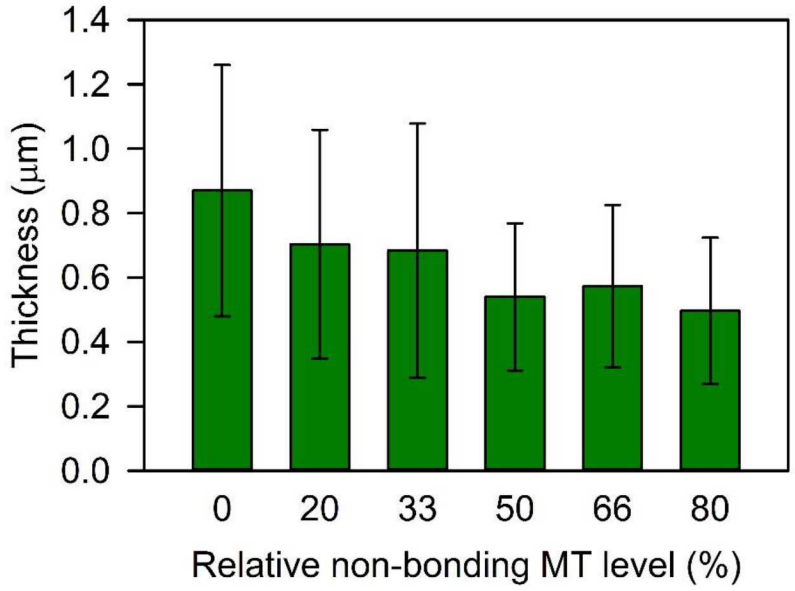

- Average thickness of spools formed by segmented MTs (20-80%) were <u>smaller</u> than spools formed by bonding MTs (0%)
- Thickness of spools <u>inversely correlated</u> with the non-bonding MT level

Non-bonding MTs hinder growth of spools

AFM and SEM of FBS-coated SAMs

glass

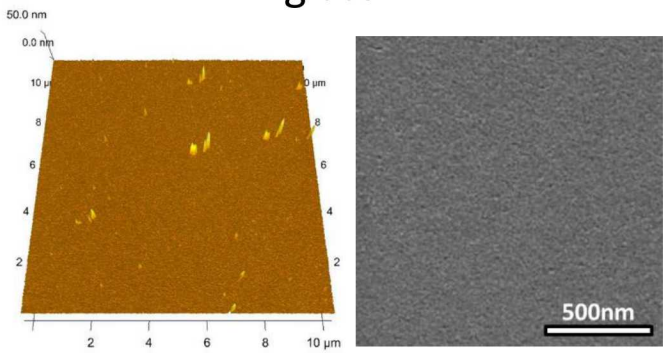

Au

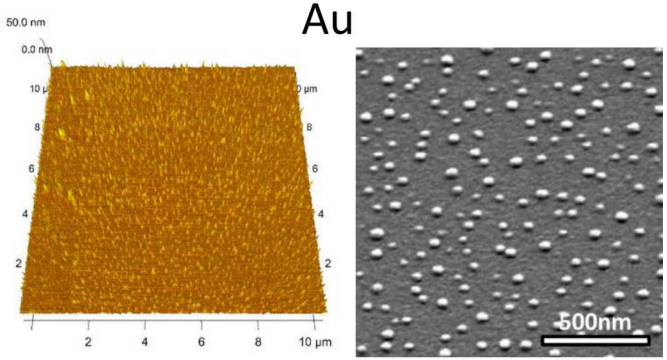

COO^-

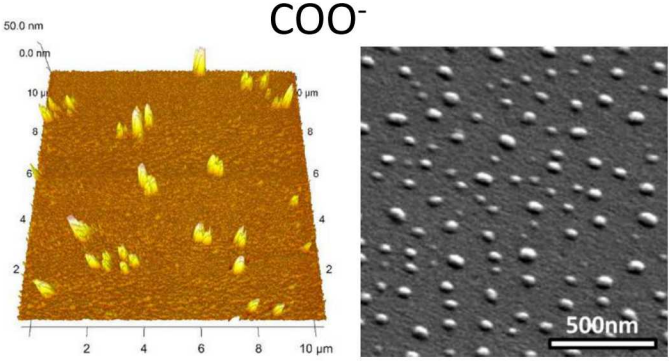

NH_3^+

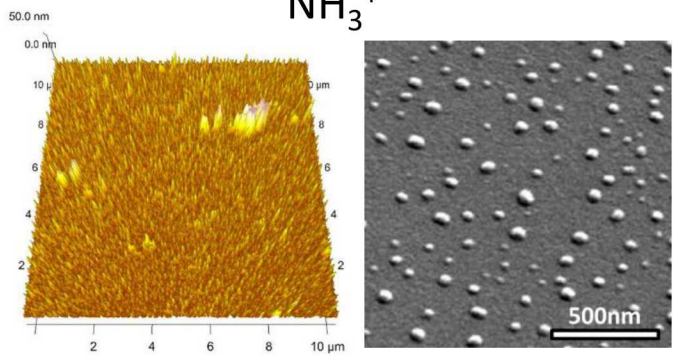

CH_3

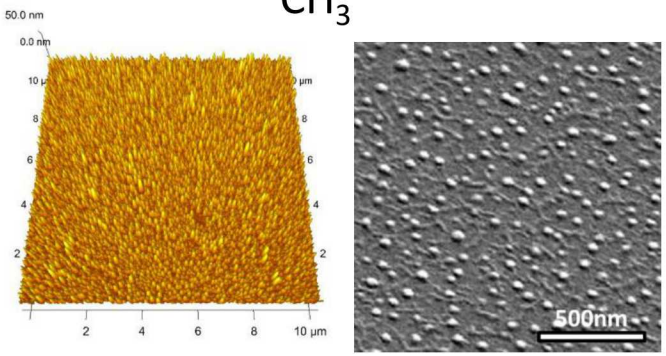

- Change in morphology compared to SAMs layer indicated protein presence on surfaces
- SEM images show round structures on surface (~ 50-70 nm)
  - More dispersed and larger on hydrophilic SAMs

Substrate roughness vs. MT velocity

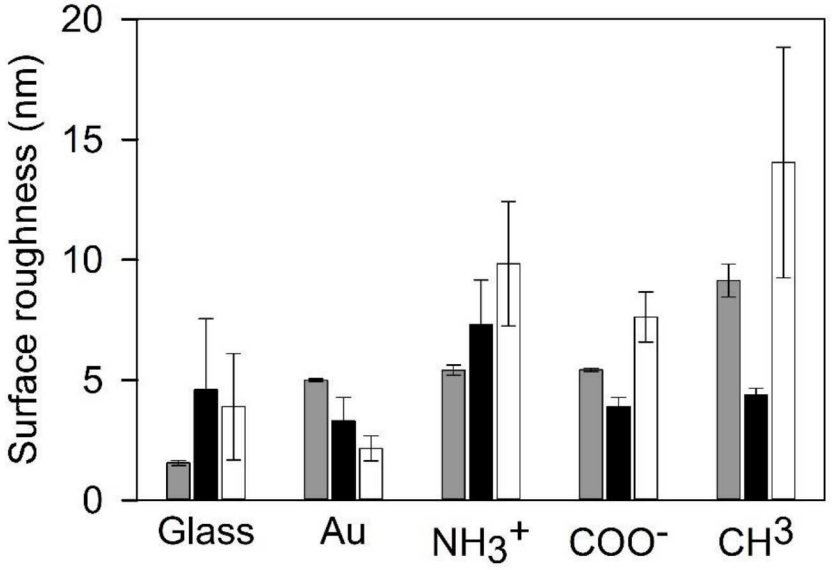

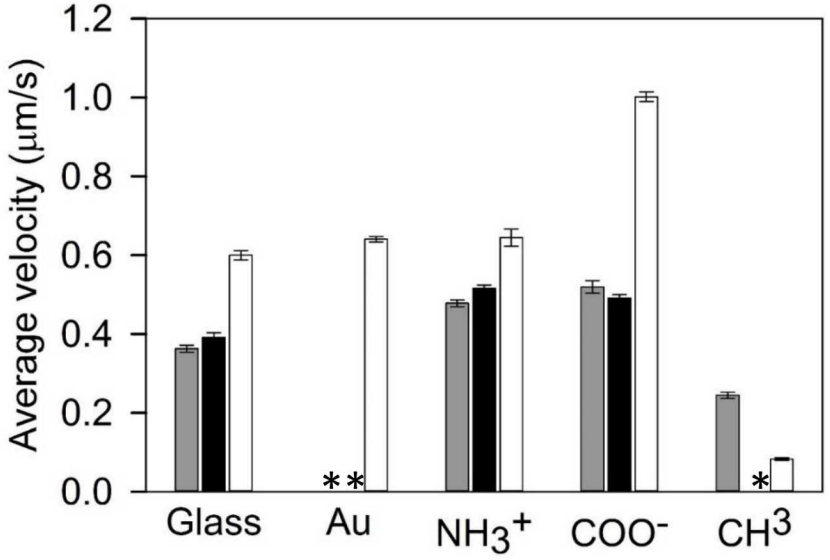

Distribution of MT velocities

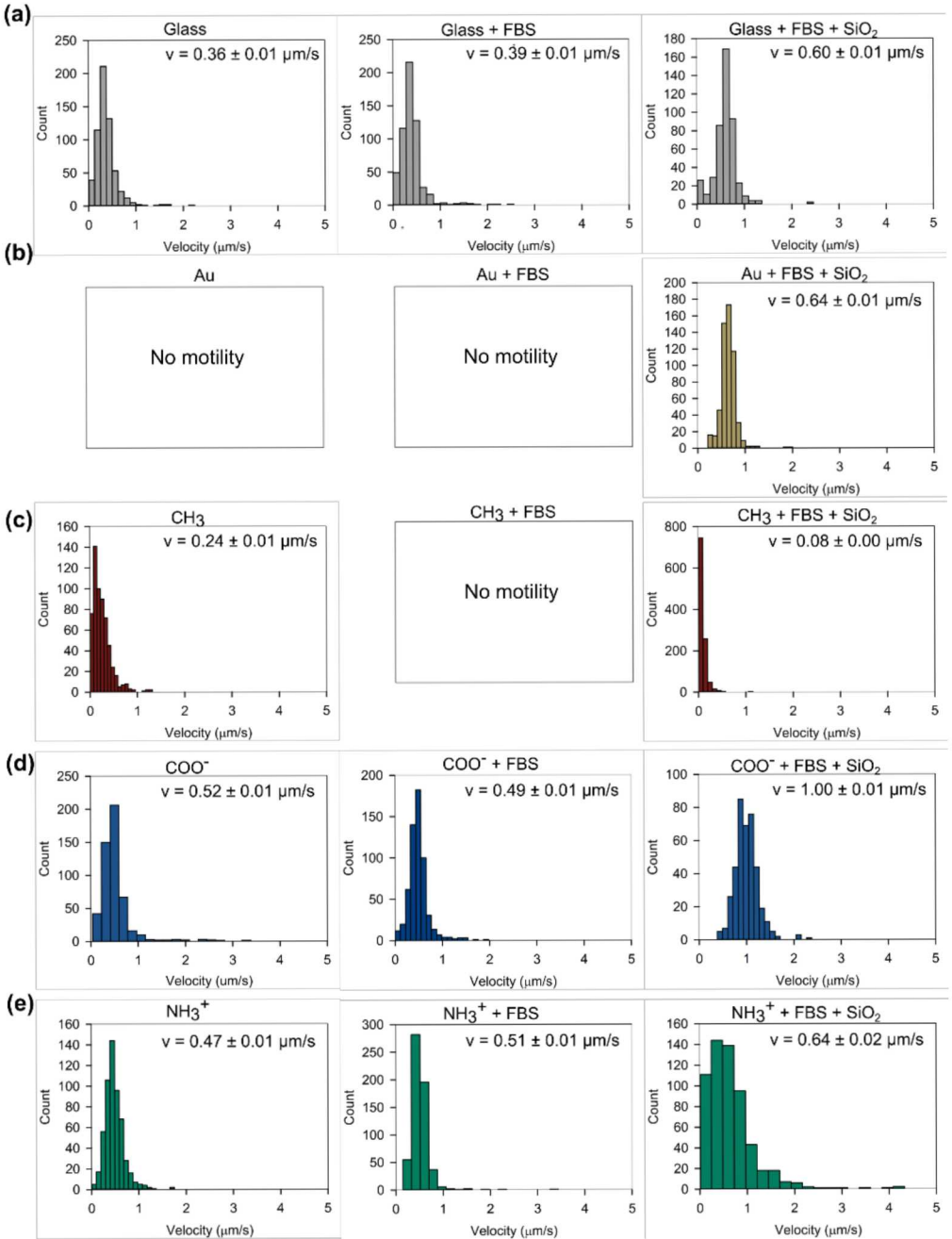

Statistical analysis of MT velocity

Substrate	Krushal-Wallis test p-value	Group comparison	Dunn's test p-value
SAMs	< 0.001	COO^- vs. CH_3	< 0.001
		COO^- vs. glass	< 0.001
		COO^- vs. NH_3^+	1.000
		NH_3^+ vs. CH_3	< 0.001
		NH_3^+ vs. glass	< 0.001
		Glass vs. CH_3	< 0.001
SAMs + FBS	< 0.001	NH_3^+ vs. glass	< 0.001
		COO^- vs. NH_3^+	0.013
		COO^- vs. glass	< 0.001
SAMs + FBS + SiO_2	< 0.001	COO^- vs. CH_3	< 0.001
		COO^- vs. glass	< 0.001
		COO^- vs. NH_3^+	< 0.001
		COO^- vs. Au	< 0.001
		NH_3^+ vs. CH_3	< 0.001
		NH_3^+ vs. glass	1.000
		Glass vs. CH_3	< 0.001
		Au vs. CH_3	< 0.001
		Au vs. NH_3^+	0.037
		Au vs. glass	0.253

Statistical analysis of MT velocity

Substrate	Group comparison	Dunn's/Mann-Whitney test p-value
glass	Glass **vs.** Glass + FBS	0.078
	Glass **vs.** Glass + FBS + SiO_2	< 0.001
	Glass + FBS **vs.** Glass + FBS + SiO_2	< 0.001
COO^-	COO^- **vs.** COO^- + FBS	1.000
	COO^- **vs.** COO^- + FBS + SiO_2	< 0.001
	COO^- + FBS **vs.** COO^- + FBS + SiO_2	< 0.001
NH_3^+	NH_3^+ **vs.** NH_3^+ + FBS	0.002
	NH_3^+ **vs.** NH_3^+ + FBS + SiO_2	< 0.001
	NH_3^+ + FBS **vs.** NH_3^+ + FBS + SiO_2	0.118
CH_3	CH_3 **vs.** CH_3 + FBS + SiO_2	< 0.001

Mechanism of kinesin “walking”

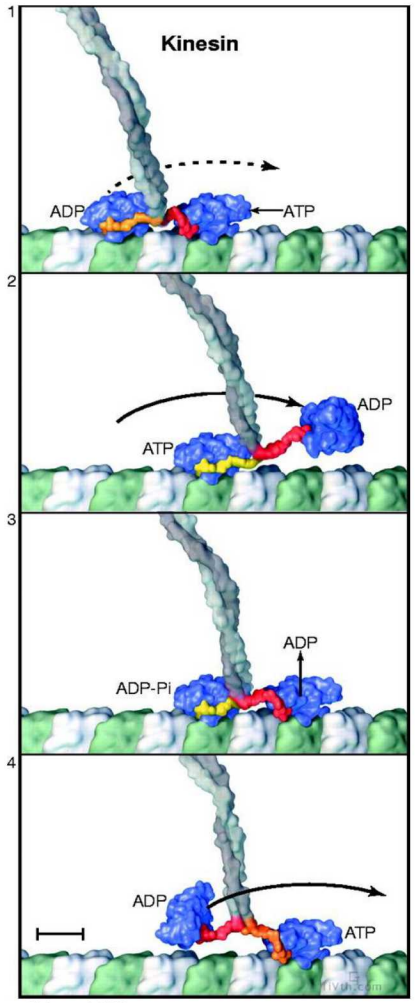

Vale et al. 2000

1) ATP binding to the leading head induces a conformational change. This power stroke causes the trailing head to move forward (towards plus end)
2) The trailing head reaches the next binding site (16 nm)
3) After a random diffusional search, the new leading head docks onto the binding site. Binding to the MT catalyzes ADP relase, and the trailing head hydrolyzes ATP to ADP-Pi.
4) ATP binds to the leading head, and realase of phosphate from the trailing head detaches the neck linker allowing the trailing head to move forward

MTs can self-heal

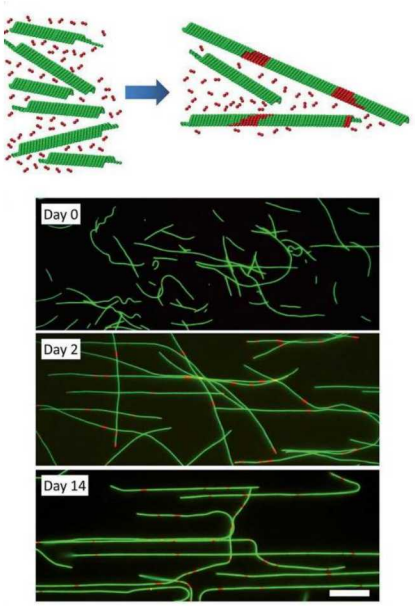

Bachand et al., RSC Adv.,2014

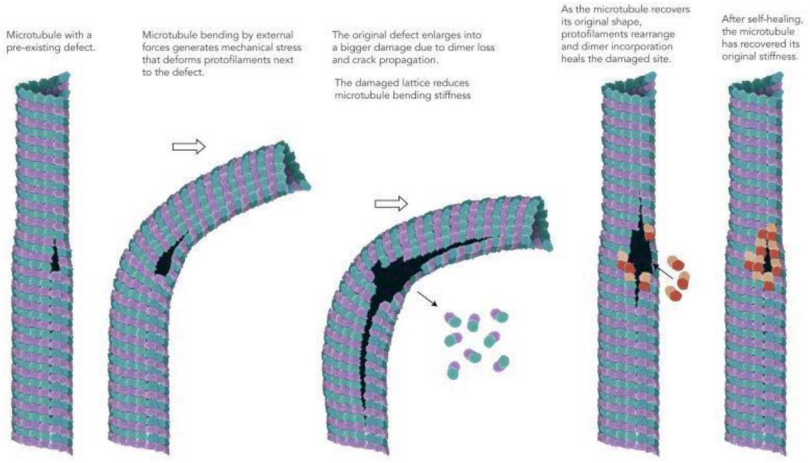

Schaedel et al., Nat Mater., 2015

MTs can self-repair mechanically induced defects in the tubulin lattice by incorporating free tubulin from solution

How are defects handled in actively assembled materials using kinesin-MT transport system?

Non-bonding MTs integrate into bonding (fully biotinylated) spool

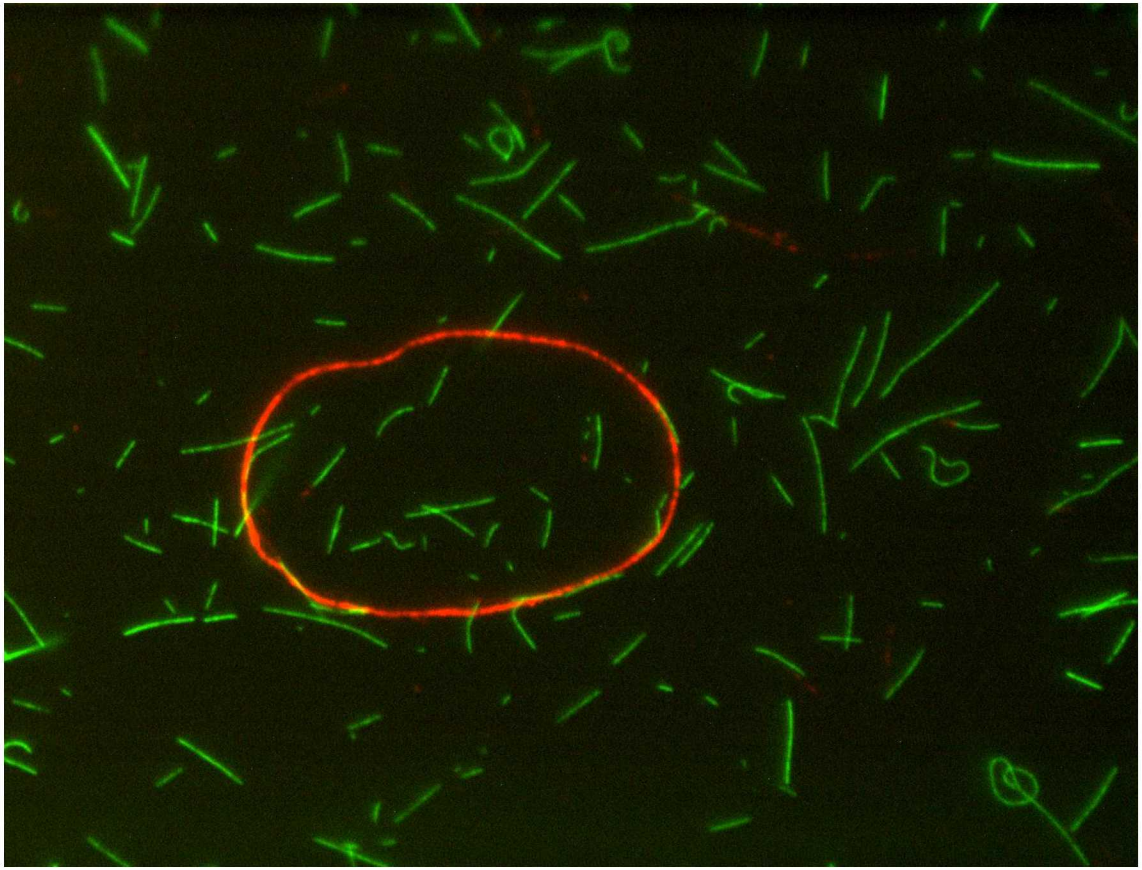

Active self assembly of rings and spools

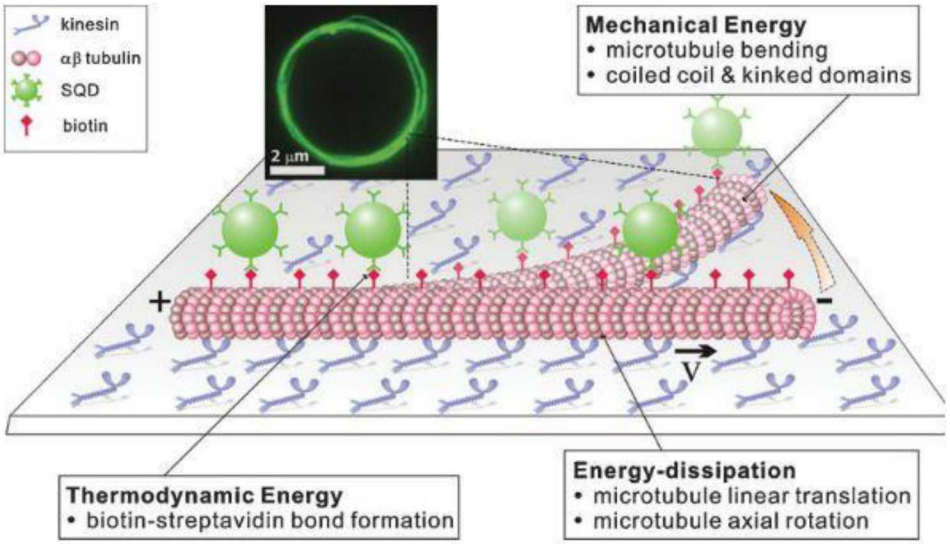

Liu et al., Advanced Materials, 2008

- Spools are actively assembled using the gliding motility geometry in which surface-adhered kinesin motors translate microtubule filaments, with attached nanoparticles, across a surface.
- kinesin motors dissipate chemical energy through ATP hydrolysis, which is coupled to the linear translation and axial rotation of microtubules
- Thermodynamic energy is added to the system through the introduction of SQDs, and the subsequent formation of biotin–streptavidin noncovalent bonds with the microtubules
- Mechanical energy is stored in the bending of the microtubule filaments, as well as the formation of coiled coil and kinked domains within the assembled structures